

GRAPPA Student Seminar



Searching for non-gravitational signatures of
Dark Matter in the Galactic Center

Oscar Macias
(Jun 11th, 2019)

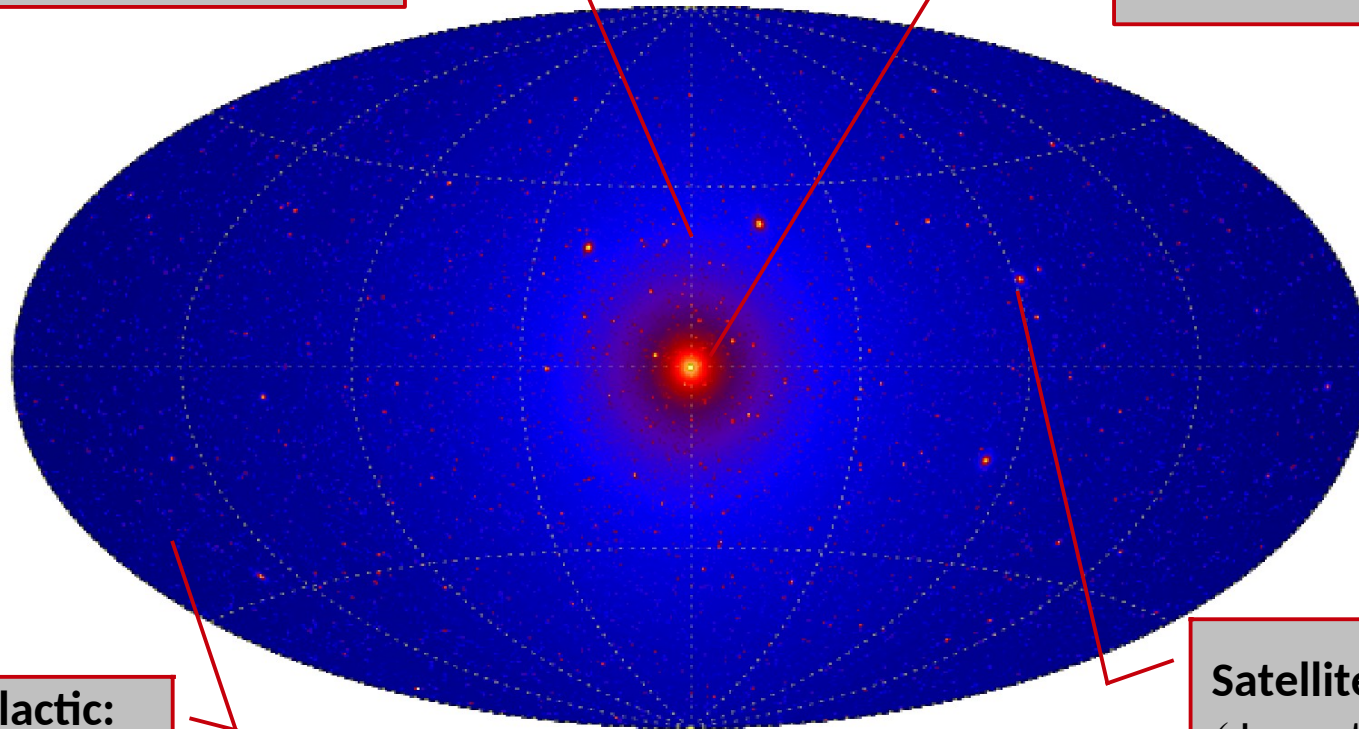
Where to look for dark matter emission?

Galactic Halo:

- ✓ Large Statistics
- ✓ Uncertain Background

Galactic Center:

- ✓ Large Statistics
- ✓ Uncertain Background



Extragalactic:

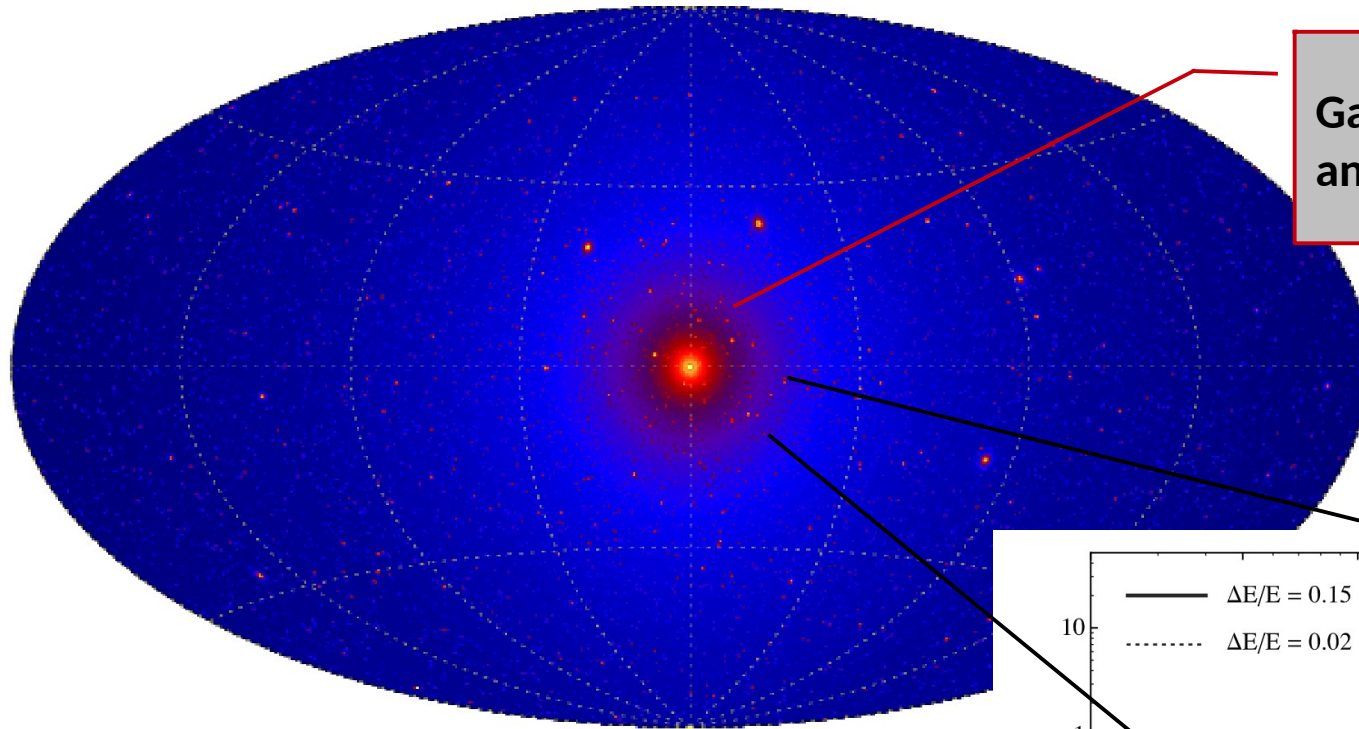
- ✓ Isotropic
- ✓ Clusters
- ✓ Uncertain background

Satellite Galaxies:

- ✓ Low statistics
- ✓ Clean background
- ✓ Uncertain DM distribution

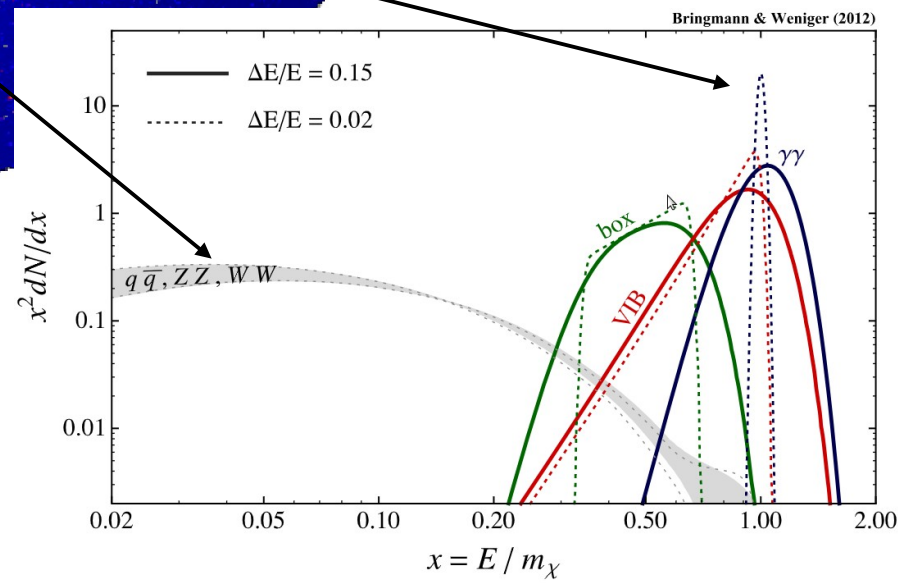
All sky map of gamma-rays from DM annihilation (Via Lactea II simulation),
arXiv:0908.0195

What would we expect to see?



(Via Lactea II simulation), arXiv:0908.0195

Galactic Center morphology
and spectrum



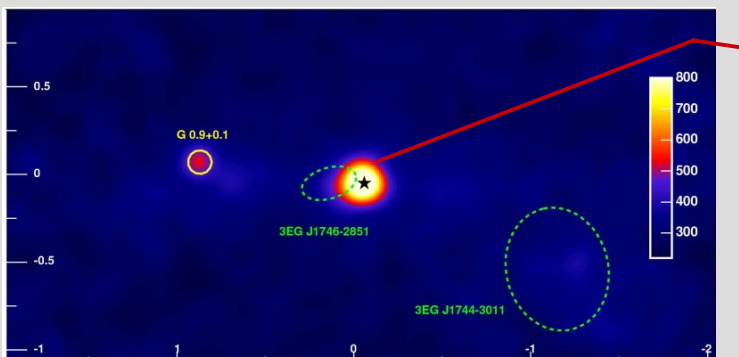
The GC should be the region displaying the brightest radiative signature of dark matter in the Galaxy



Image Credit: C. Crockett

Remarkable Non-Thermal Phenomena of the Galactic Center/Inner Galaxy

1) The (quasi) point-like GeV-TeV source Sgr A*:

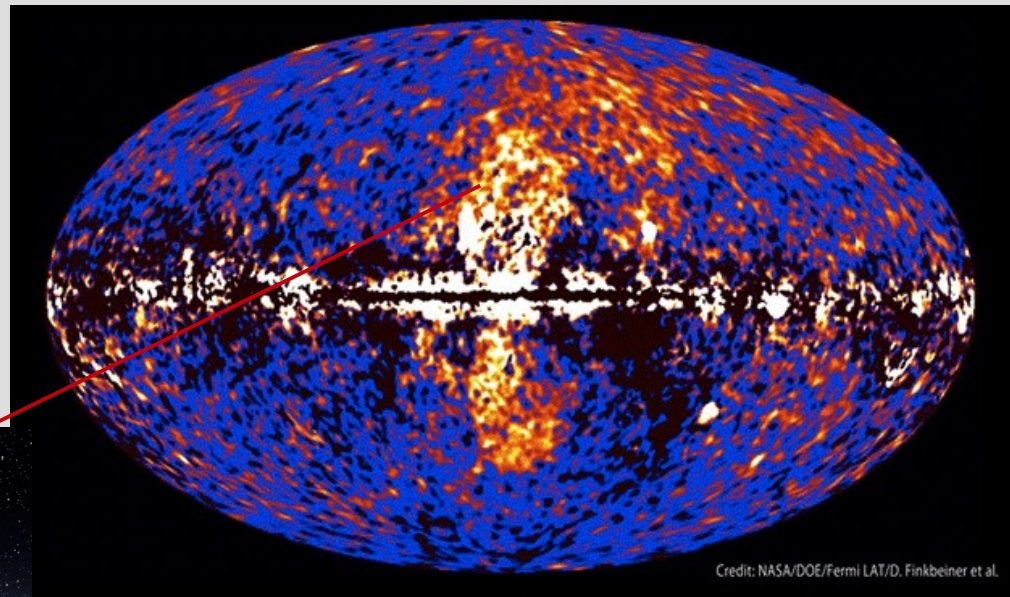
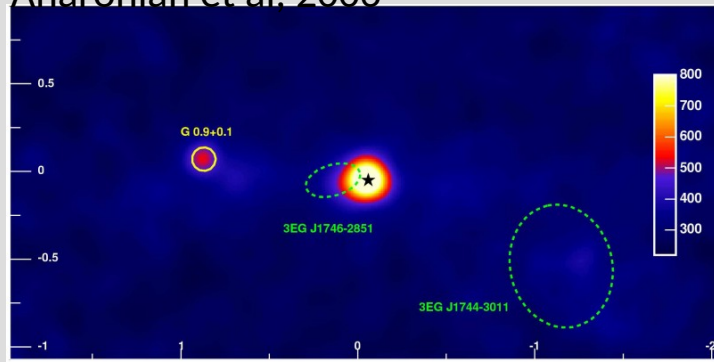


- ✓ Complex spectrum with spectral bumps in the 1 GeV – 10 TeV energy range.
- ✓ Active Galactic Nuclei (AGN) emission
- ✓ Attributed to dark matter annihilation in e.g. arxiv:1207.2412

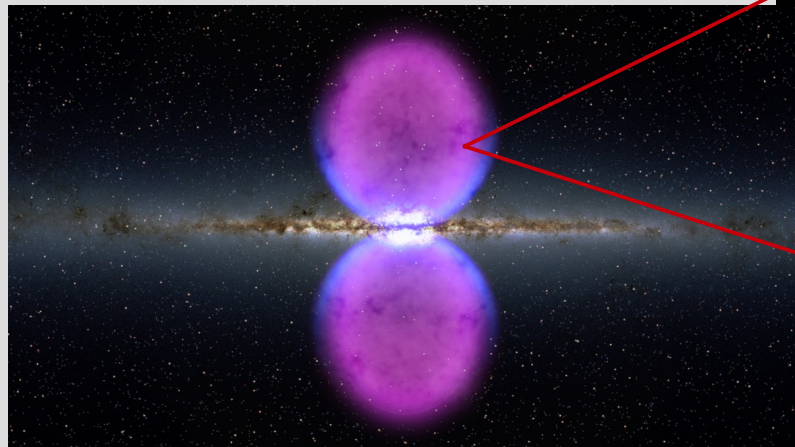
Remarkable Non-Thermal Phenomena of the Galactic Center/Inner Galaxy

1) The (quasi) point-like GeV-TeV source Sgr A*:

Aharonian et al. 2006



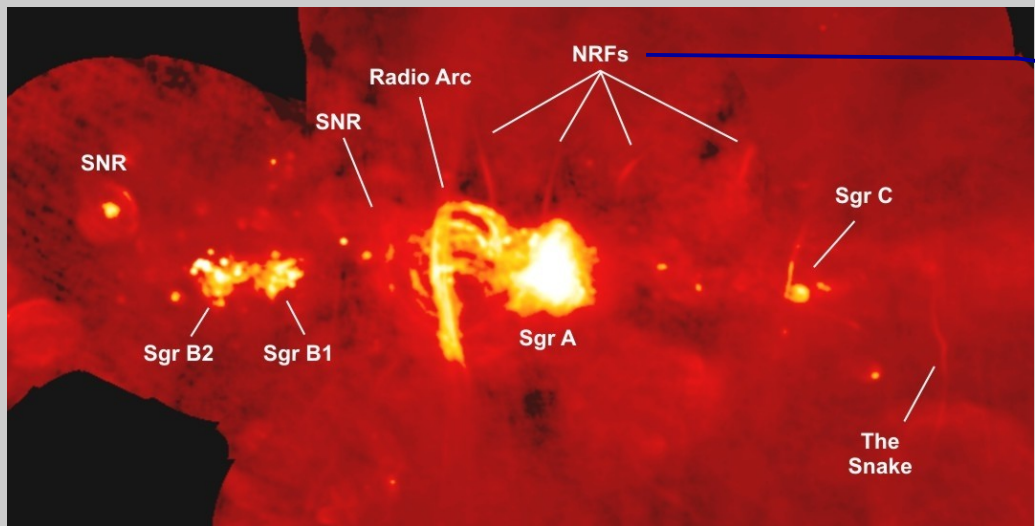
2) The Fermi Bubbles:



- ✓ Large scale non-thermal structures
- ✓ Extend up to ~60 deg in latitude
- ✓ Found counterparts in X-ray, radio and microwaves
- ✓ Attributed to dark matter annihilation in e.g. arxiv:0705.3655 (!)

Remarkable Non-Thermal Phenomena of the Galactic Center/Inner Galaxy

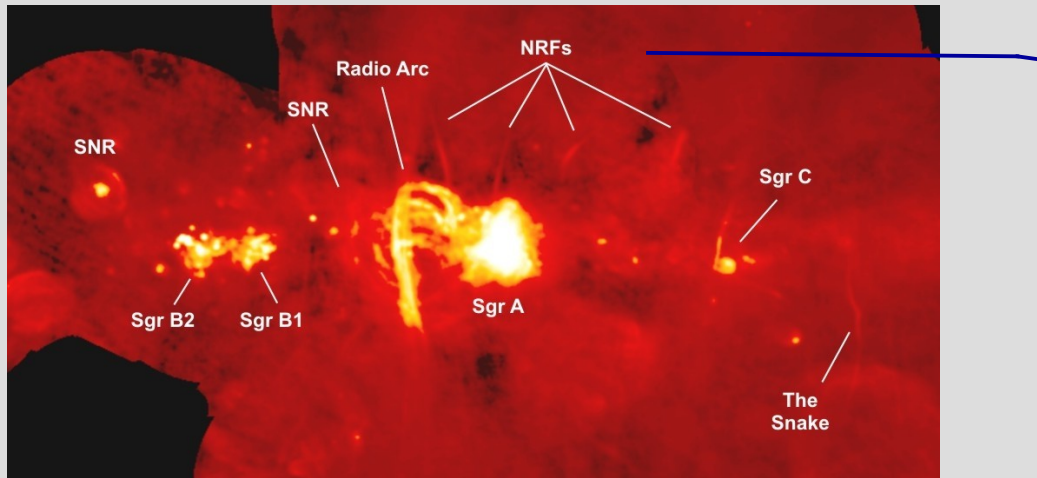
3) Non-Thermal Radio (and X-ray) Filaments (NRFs):



- ✓ Observed in radio with VLA and GBT telescopes
- ✓ Thought to be pockets of starburst activity
- ✓ Attributed to DM annihilation in e.g. arxiv:1106.5993 (!)

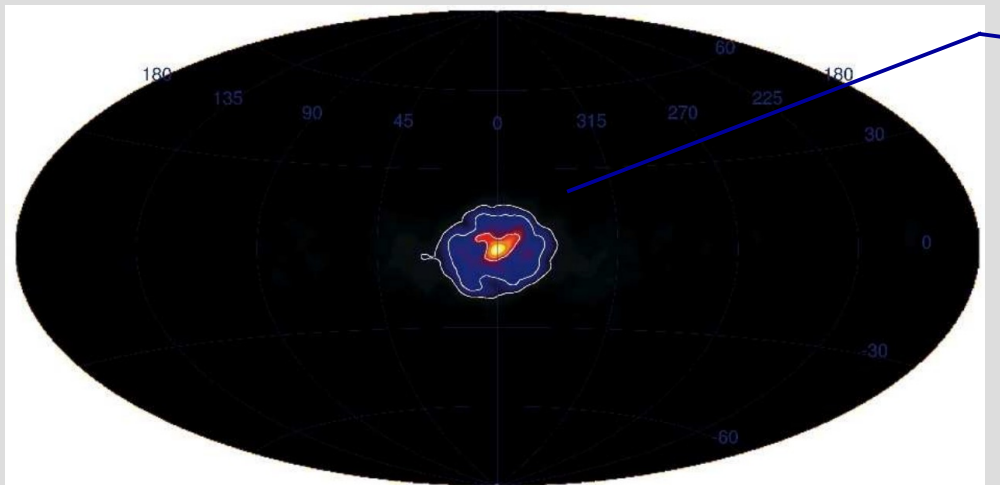
Remarkable Non-Thermal Phenomena of the Galactic Center/Inner Galaxy

3) Non-Thermal Radio (and X-ray) Filaments (NRFs):



- ✓ Observed in radio with VLA and GBT telescopes
- ✓ Thought to be pockets of starburst activity
- ✓ Attributed to DM annihilation in e.g. arxiv:1106.5993 (!)

4) The 511 keV positron annihilation line:



- ✓ Strong peak close to sgr A*
- ✓ Injection of 2×10^{42} e+/s
- ✓ Extend up to 10 deg in latitude
- ✓ Attributed to DM annihilation in e.g. arxiv:1710.03906 (!)

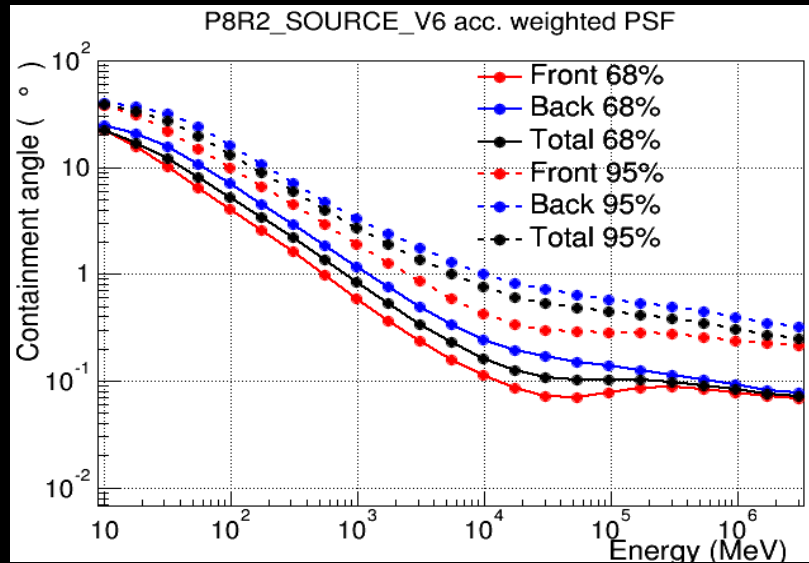
Intermezzo

It is remarkable that every single one of these phenomena has been claimed as potential evidence of a dark matter-related processes.

Extreme caution must be exercised in adducing an unusual GC signal as evidence for a dark matter initiated Processes.

Searches for Dark Matter emission with the Fermi Gamma-ray Space Telescope

- Fermi-LAT is a space based gamma-ray detector with an effective energy range of 20 MeV-500 GeV.
- Effective Area
- Field of view ~2.4 sr
- Energy resolution ~10%
- Angular resolution is energy dependent



Galactic Center Excess (GCE)

From the Galactic Center
out to mid-latitudes

Goodenough & Hooper (2009)

Vitale & Morselli (2009)

Hooper & Goodenough (2011)

Hooper & Linden (2011)

Boyarsky et al (2011)

Abazajian & Kaplinghat (2012)

Gordon & Macias (2013)

Hooper & Slatyer (2013)

Huang et al (2013)

Macias & Gordon (2014)

Abazajian et al (2014, 2015)

Calore et al (2014)

Zhou et al (2014)

Daylan et al (2014)

Selig et al (2015)

Huang et al (2015)

Gaggero et al (2015)

Carlson et al (2015, 2016)

Yand & Aharonian (2016)

Horiuchi et al (2016)

Lee et al (2016)

Bartels et al (2016)

Linden et al (2016)

Ackermann et al (2017)

Ajello et al (2017)

Macias et al (2017)

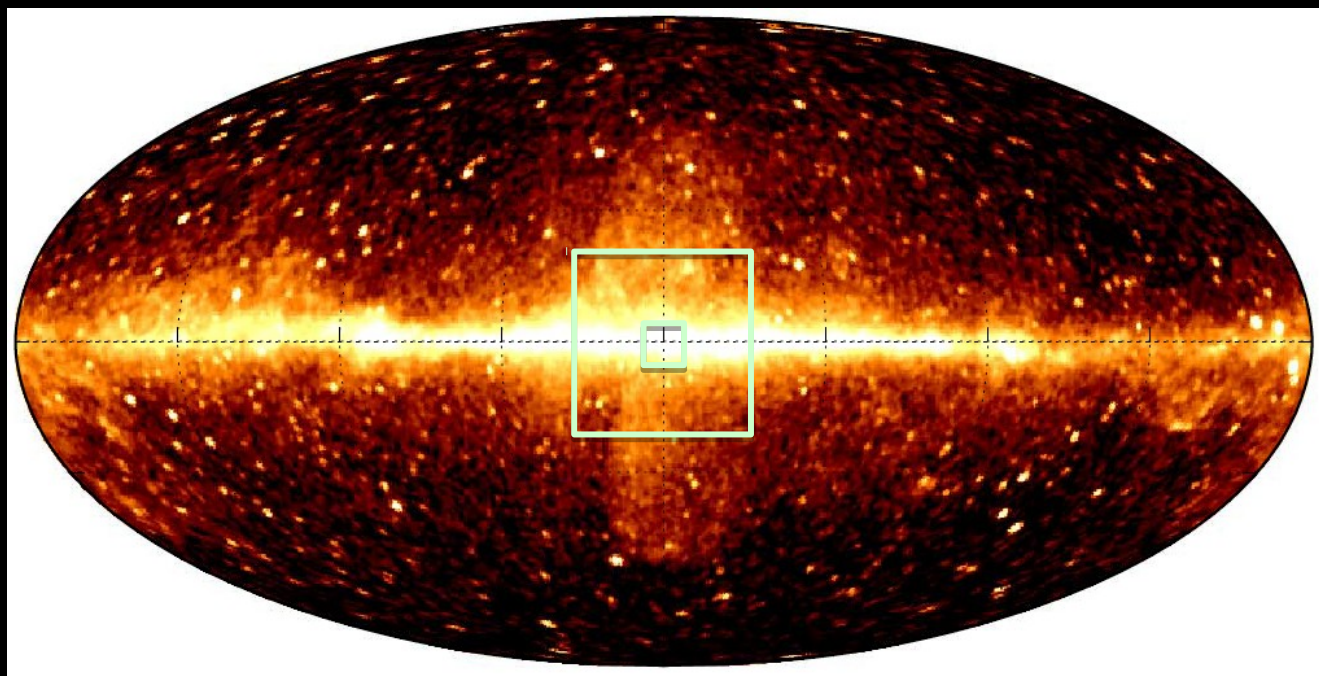
Bartels et al (2017)

...

(not a complete list)

Method

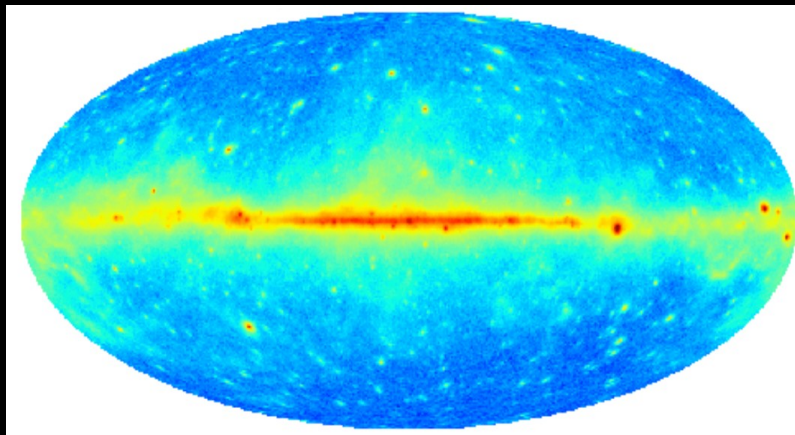
Found by morphological template fitting



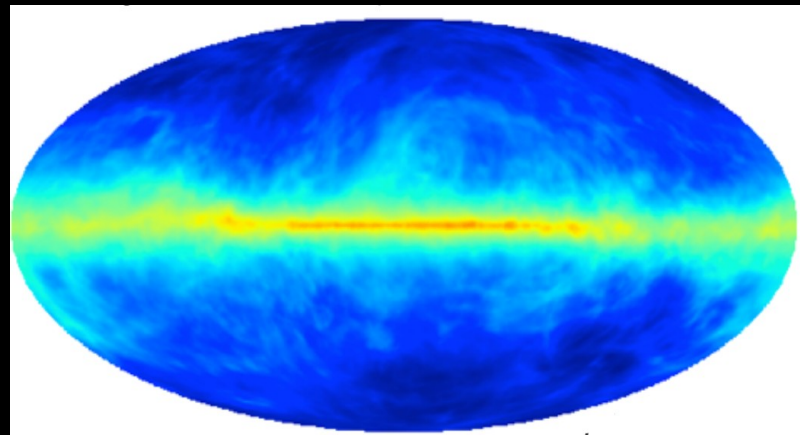
Fermi (2017)

Modeling strategy: template fitting

Data



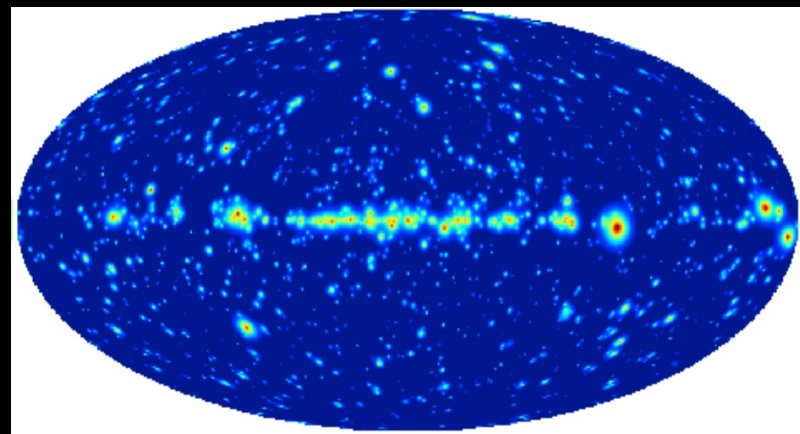
Galactic diffuse emission



=

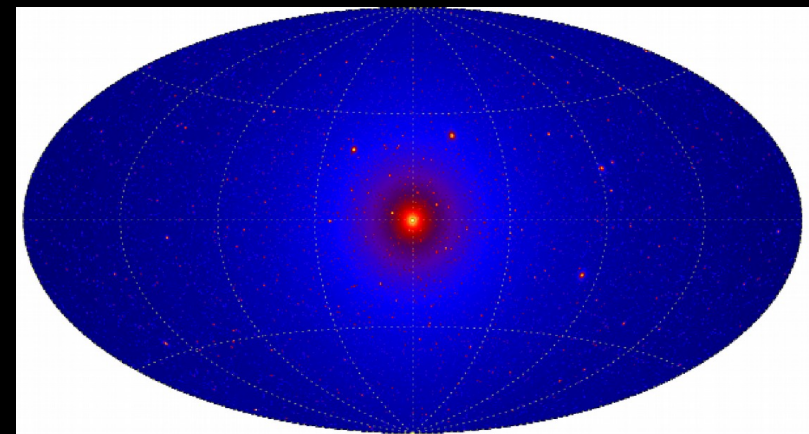
+

Known sources



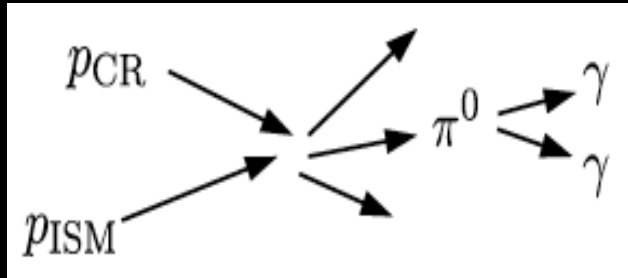
+

New sources, e.g., dark matter

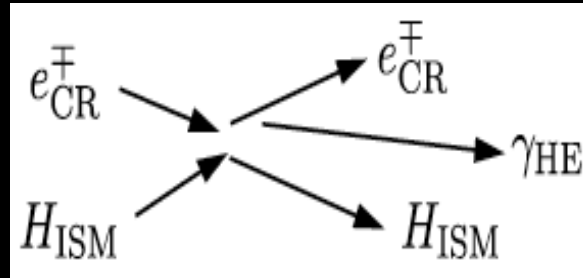


Galactic Diffuse Emission

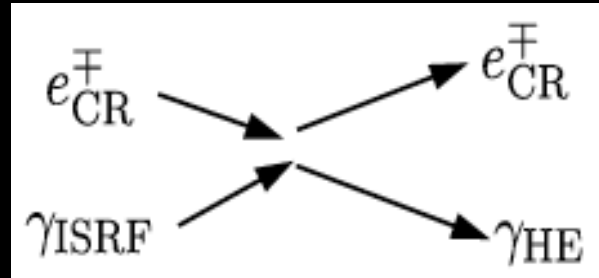
Decay of neutron pions



Bremsstrahlung



Inverse Compton



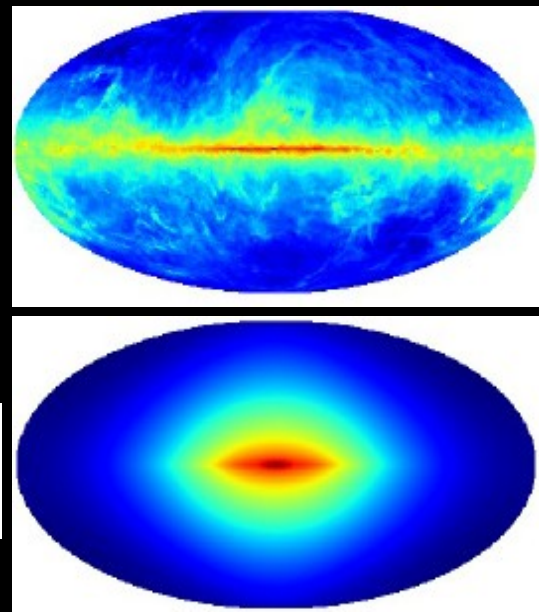
Simulations

Numerically solve the diffusion equation, e.g., Galprop

- ✓ Allows physical parameter choices
- ✓ Can be tuned to the Galactic Center
- ✗ Many parameters not well known
- ✗ Still missing some physics
- ✗ Still poor resolution

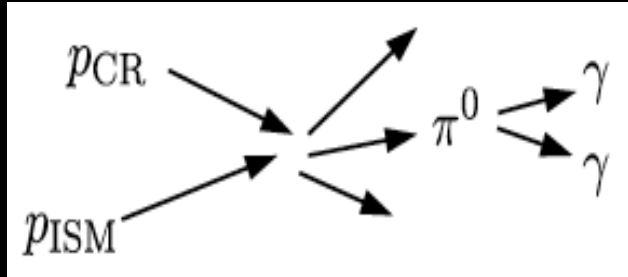
$$\frac{\partial \psi}{\partial t} = q(\vec{r}, p) + \vec{\nabla} \cdot (D_{xx} \vec{\nabla} \psi - \vec{V} \psi) + \frac{\partial}{\partial p} p^2 D_{pp} \frac{\partial}{\partial p} \frac{1}{p^2} \psi - \frac{\partial}{\partial p} \left[\dot{p} \psi - \frac{p}{3} (\vec{\nabla} \cdot \vec{V}) \psi \right] - \frac{1}{\tau_f} \psi - \frac{1}{\tau_r} \psi$$

e.g., Galprop; Moskalenko & Strong (1998)

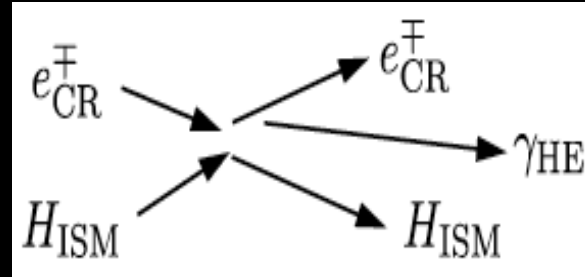


Galactic Diffuse Emission

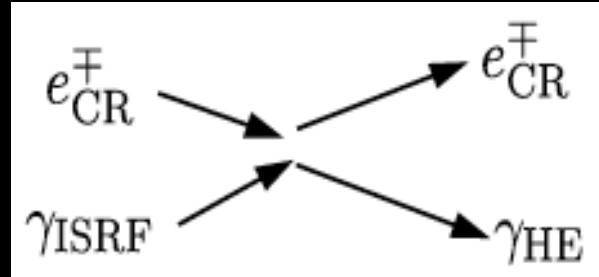
Decay of neutron pions



Bremsstrahlung



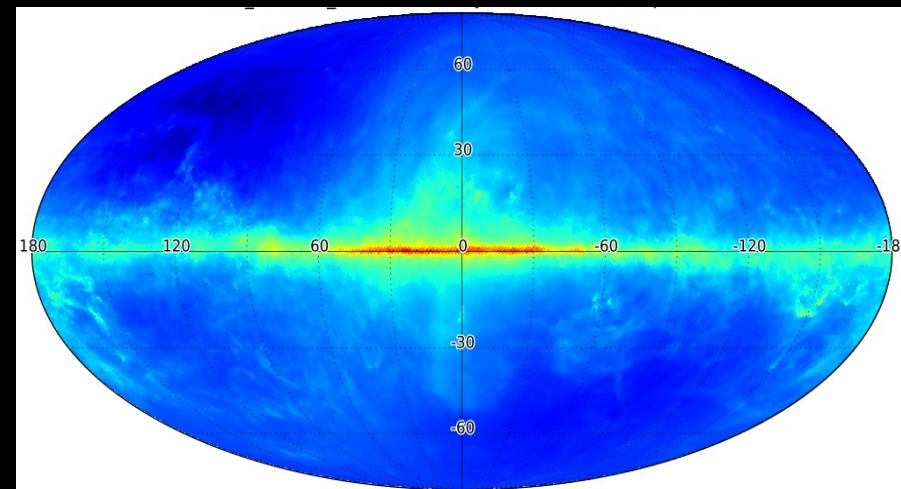
Inverse Compton



Fermi diffuse map

Built for all-sky, starting with many templates split into annuli

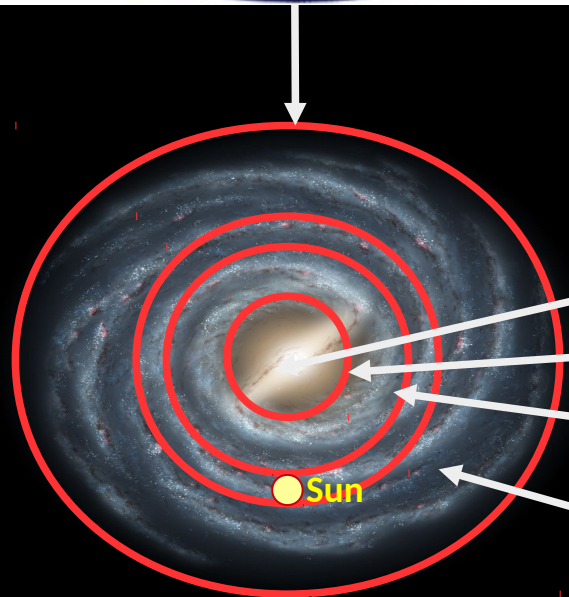
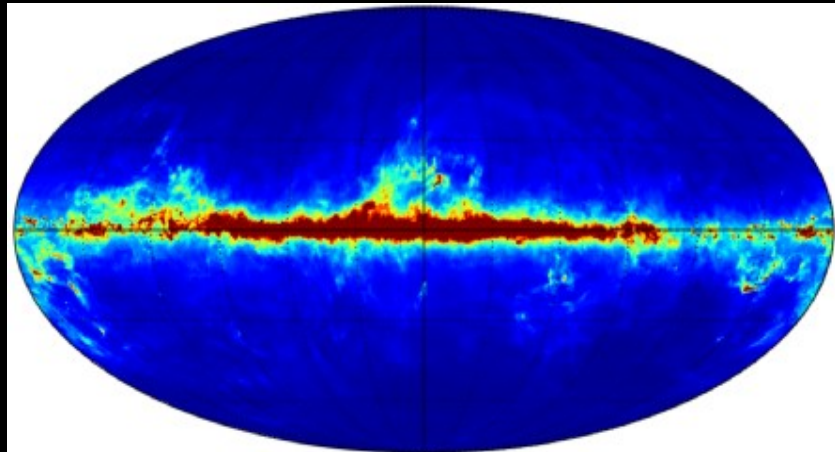
- ✓ Simple (hard work already done!)
- ✓ Accounts for some cosmic-ray injection and propagation variations (via annuli)
- ✗ Somewhat of a black box for user
- ✗ Fixed to (usually) older data
- ✗ Not dedicated for the GC.



Acero et al (2016)

Atomic and Molecular Hydrogen

Gas correlated photons
(Neutral Pion and Bremsstrahlung)



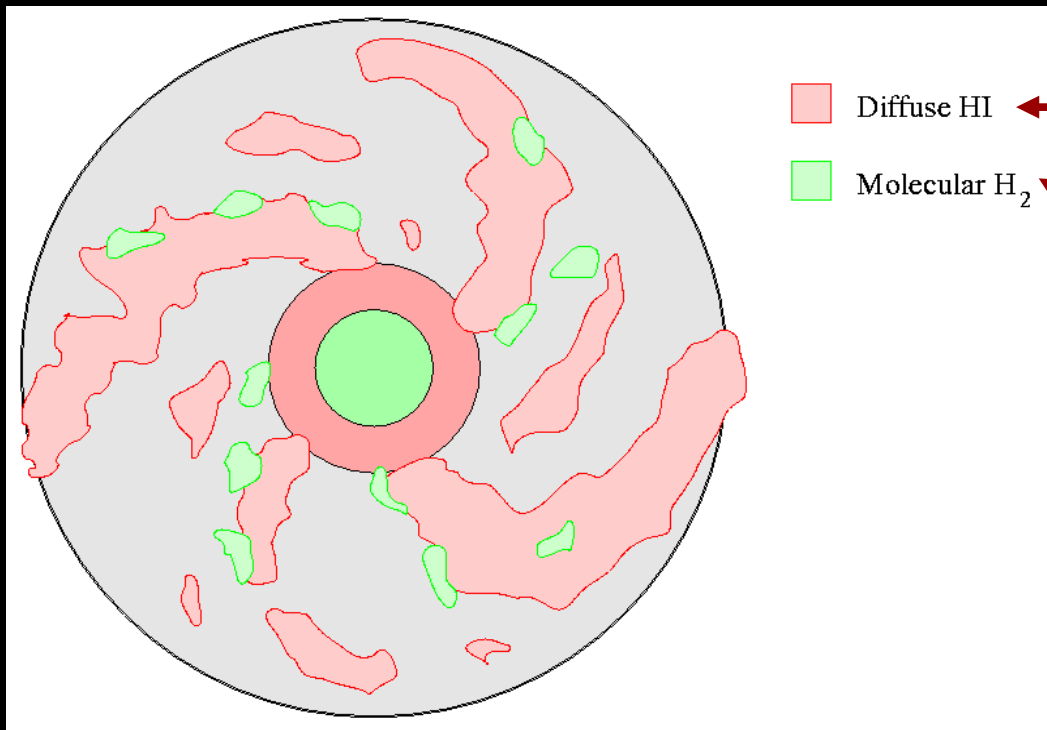
Annulus 1: 0 – 3.5 kpc

Annulus 2: 3.5 – 8.0 kpc

Annulus 3: 8.0 – 10.0 kpc

Annulus 4: 10.0 – 50.0 kpc

Atomic and Molecular Hydrogen

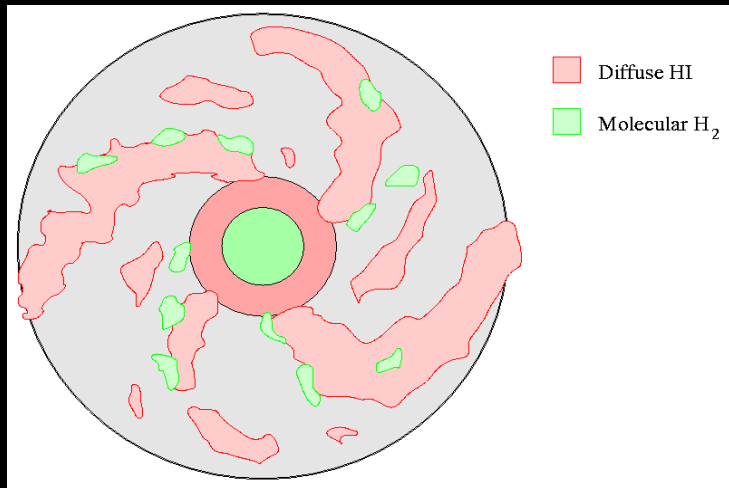


LAB Survey
[Kalberla et.al.(2005)]

Center for Astrophysics
[Dame et.al.(2000)]

→ { HI is measured with 21-cm emission
H₂ is traced by 2.6-mm line emission of CO

Annuli gas decomposition



Astronomical Surveys

Gas Cloud Velocity

Gas Cloud Temperature

Annuli gas decomposition

Image Credit:http://spiff.rit.edu/classes/phys230/lectures/ism_gas/ism_gas.html

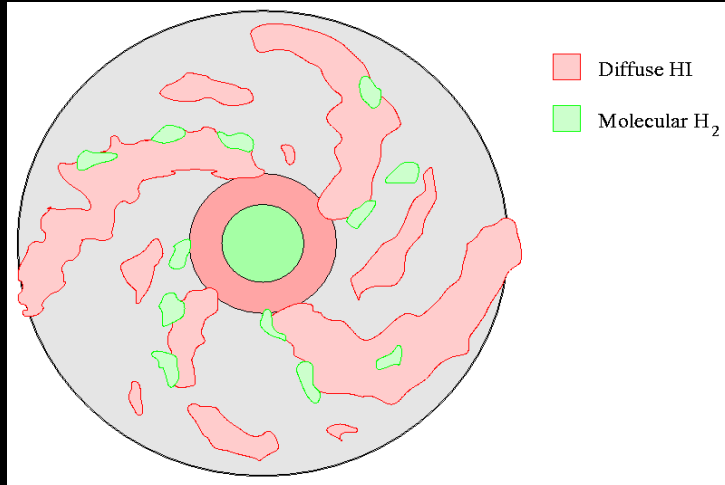
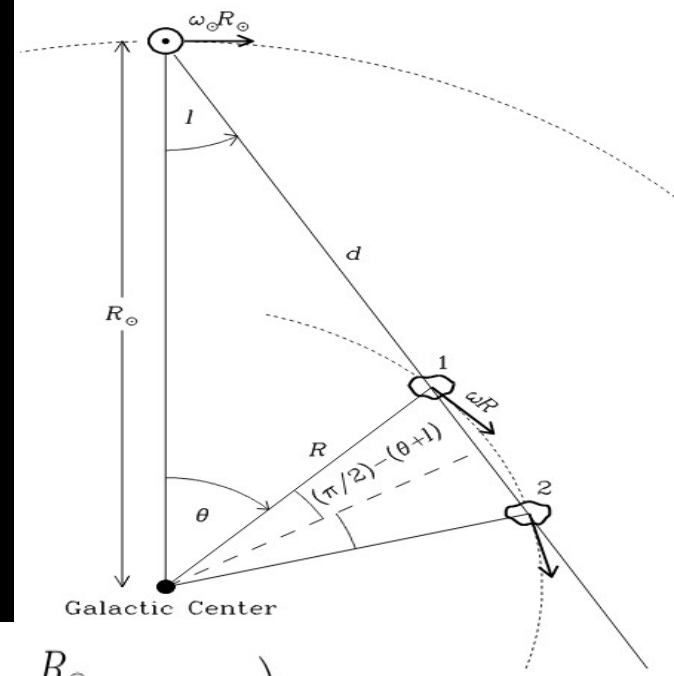


Image Credit:<http://www.cv.nrao.edu/course/astr534/HILine.html>



Astronomical Surveys

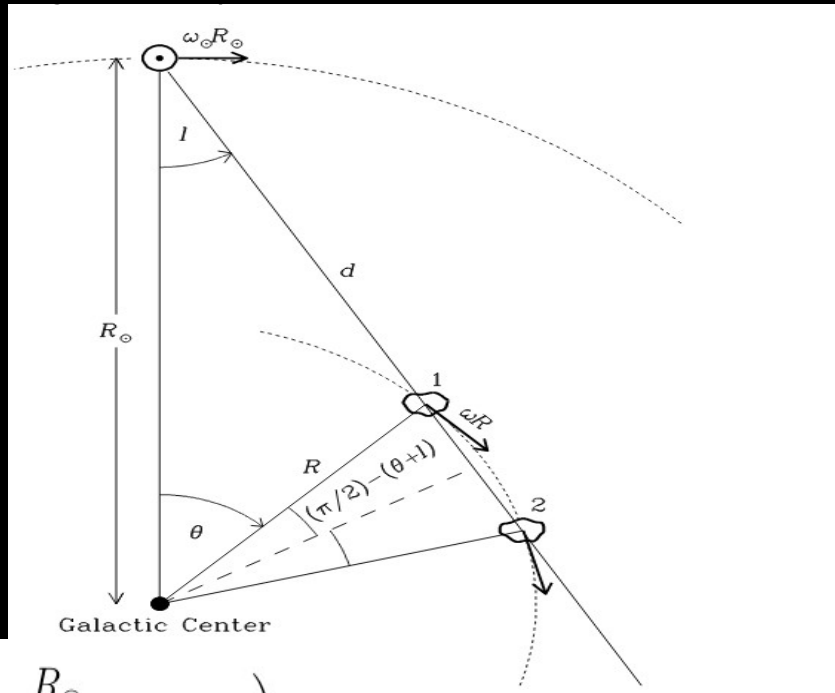
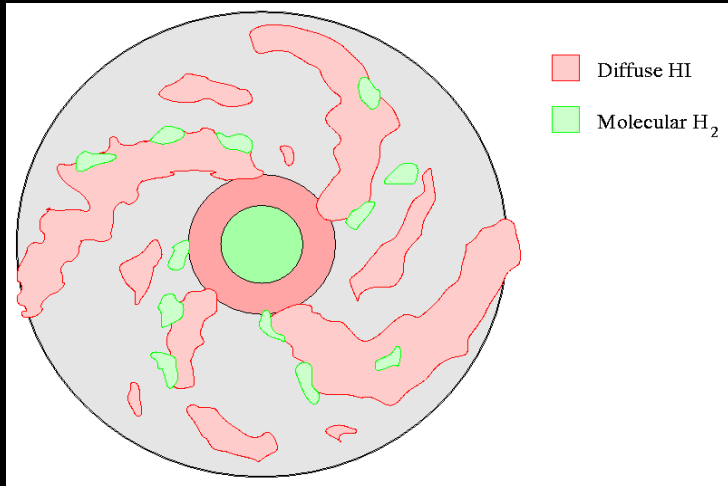
Gas Cloud Velocity

$$V_{\text{LSR}} = \left(V(R) \frac{R_\odot}{R} - V(R_\odot) \right) \sin(l) \cos(b),$$

**Gas Cloud
distance**

Gas Cloud Temperature

Annuli gas decomposition



Astronomical Surveys

Gas Cloud Velocity

$$V_{\text{LSR}} = \left(V(R) \frac{R_{\odot}}{R} - V(R_{\odot}) \right) \sin(l) \cos(b),$$

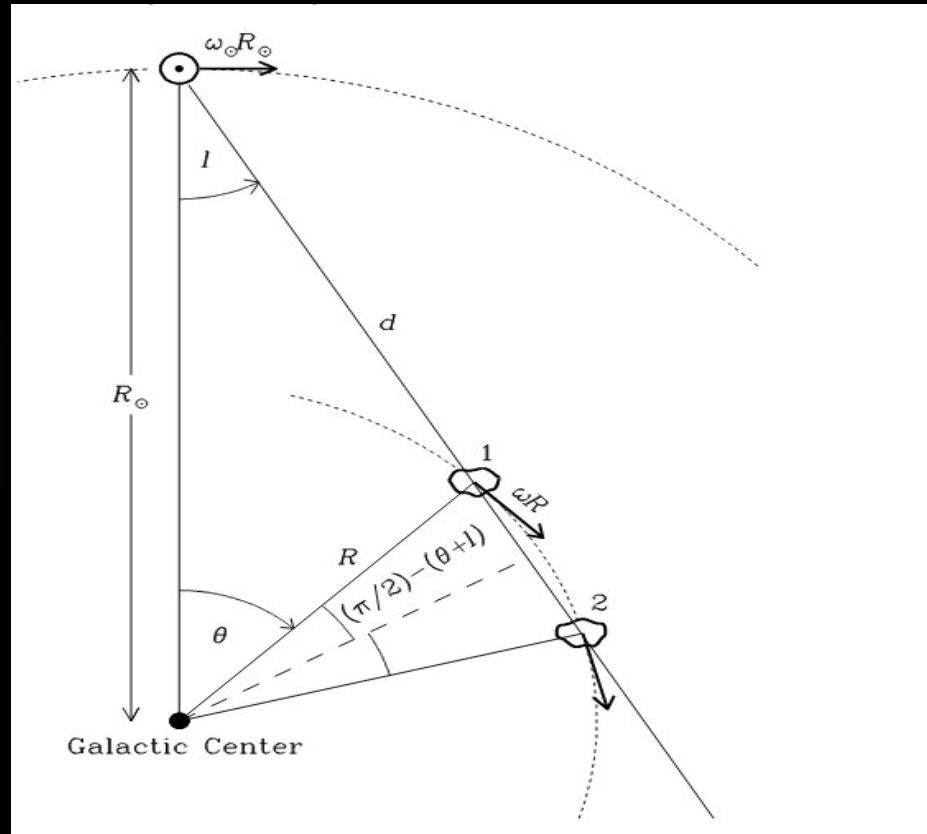
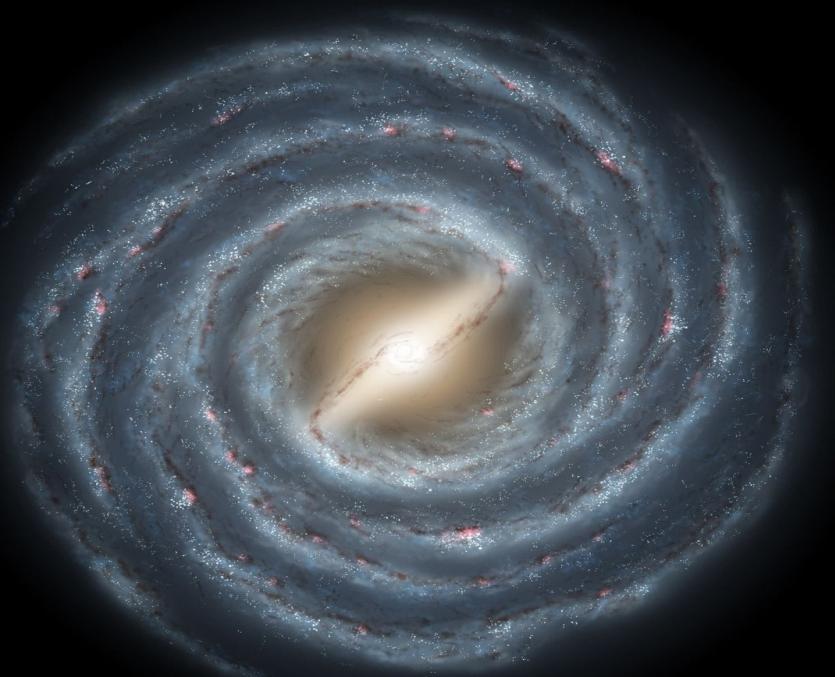
Gas Cloud distance

$$N(\text{HI}) = -C T_s \int dv \log \left(1 - \frac{T_B(v)}{T_s - T_{\text{bg}}} \right)$$

Gas Cloud Temperature

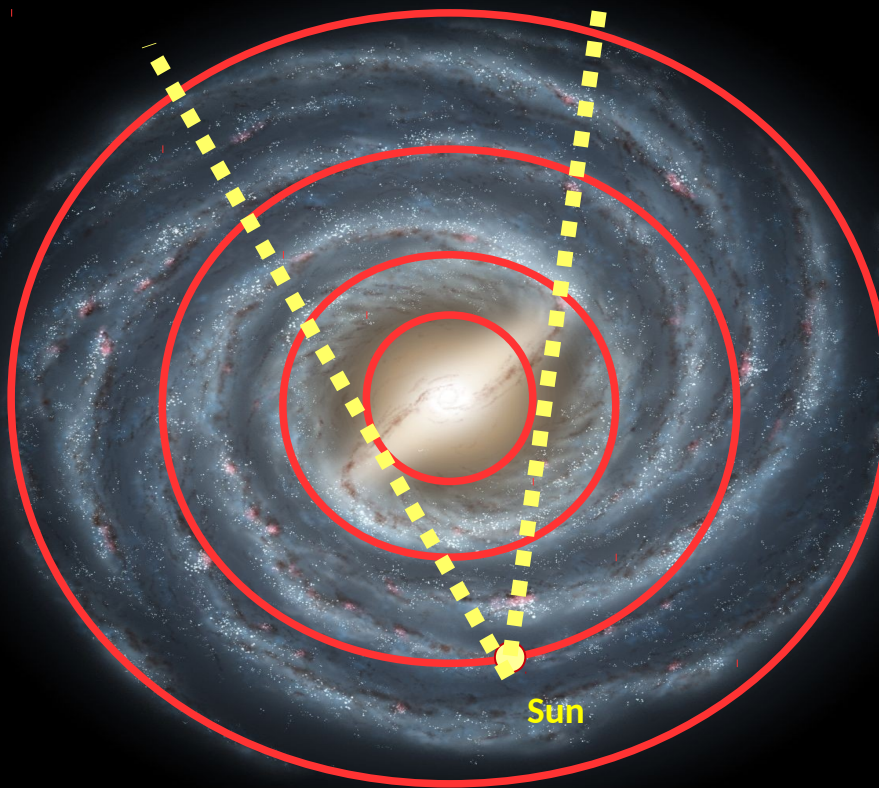
Gas Cloud density

Annuli gas decomposition



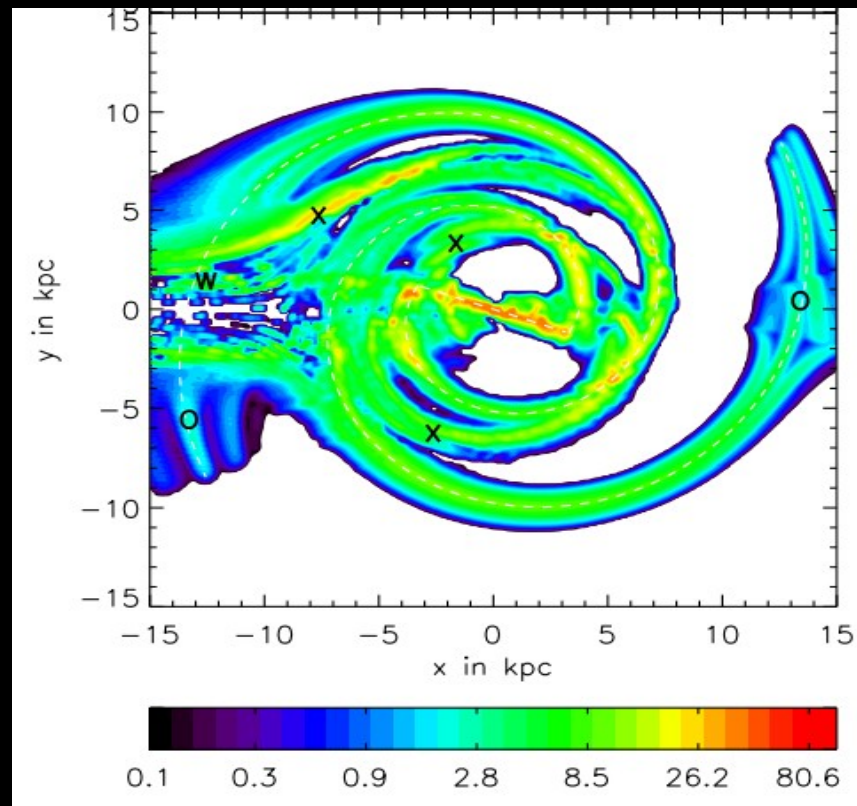
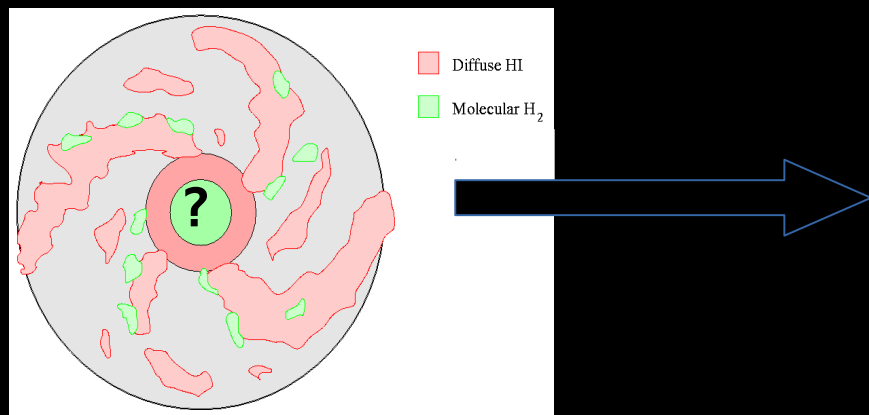
The assumption of circular motion toward the Galactic Center is incorrect!

(1) Interpolation Method



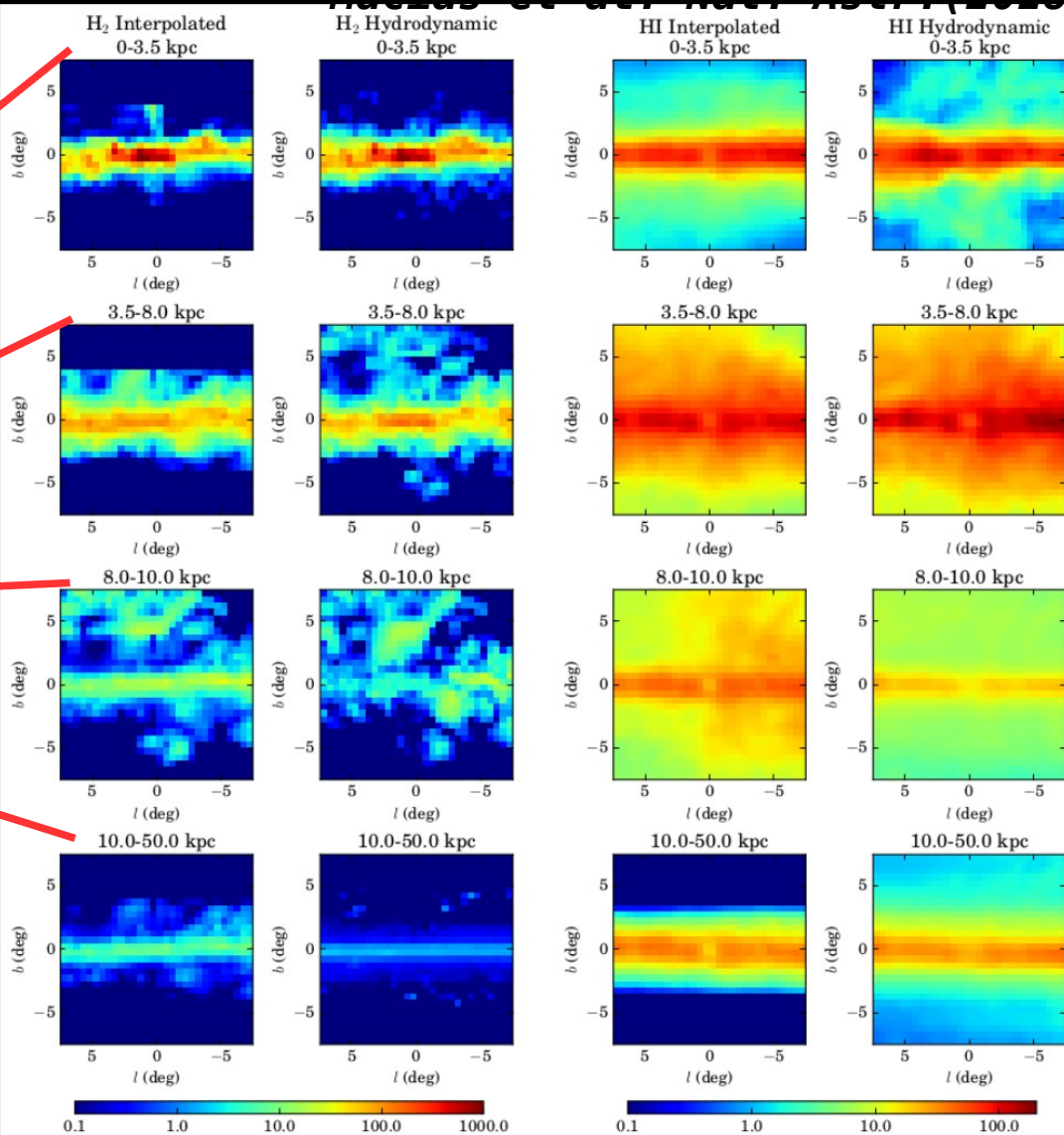
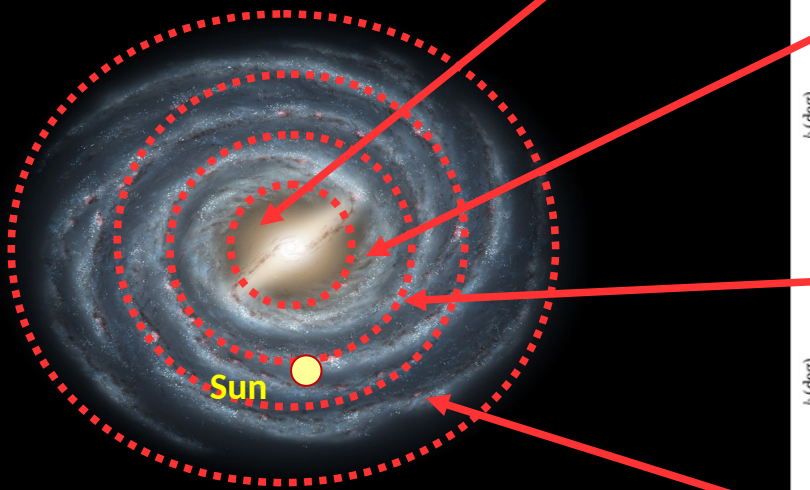
→ { Fermi-LAT uses an interpolation to estimate
the ISM gas for $10 > \text{longitude} > -10$ degrees.

(2) Hydrodynamical Simulations (this work)



Hydrodynamical simulations provide kinematic resolution toward the Galactic Center.

Interpolated vs Hydrodynamical method



There are noticeable morphological differences between the two methods.

Source templates

Known source template

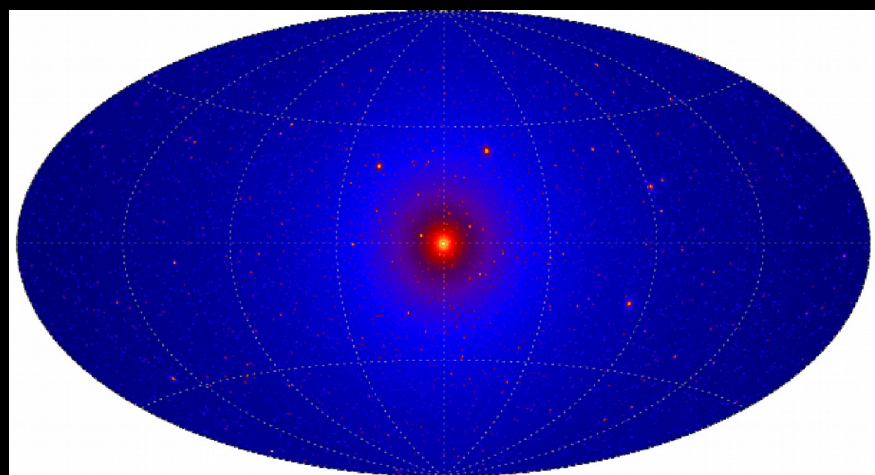
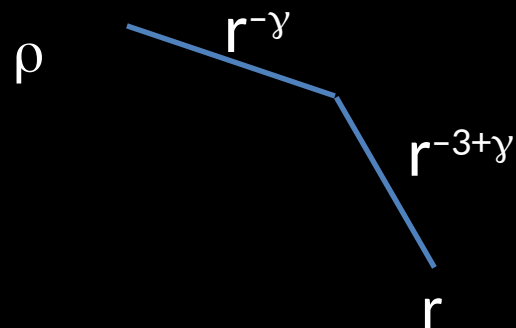
List of known point and extended sources,
e.g., Sgr A*, Fermi bubbles, loop I



New physics template

“generalized” NFW-squared template, which
allows for cosmological simulation info with
parameterized contraction effects

$$\rho \propto \left(\frac{r}{r_s}\right)^{-\gamma} \left(1 + \frac{r}{r_s}\right)^{-3+\gamma}$$



Results

The dark matter template is detected in excess wrt to

- Galactic diffuse models
- Gamma-ray emission from Sgr A*
- Other catalog & new point sources

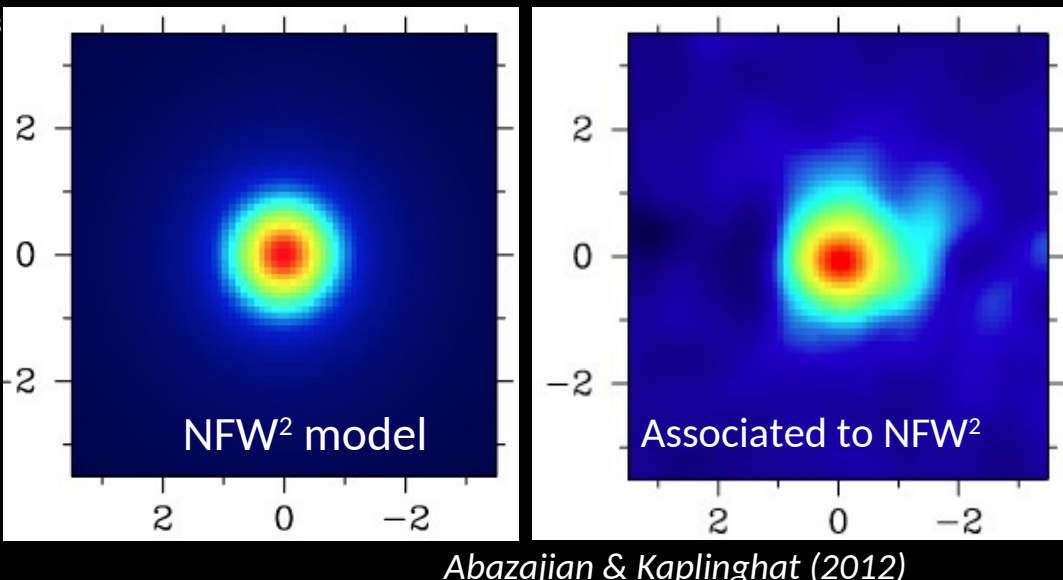
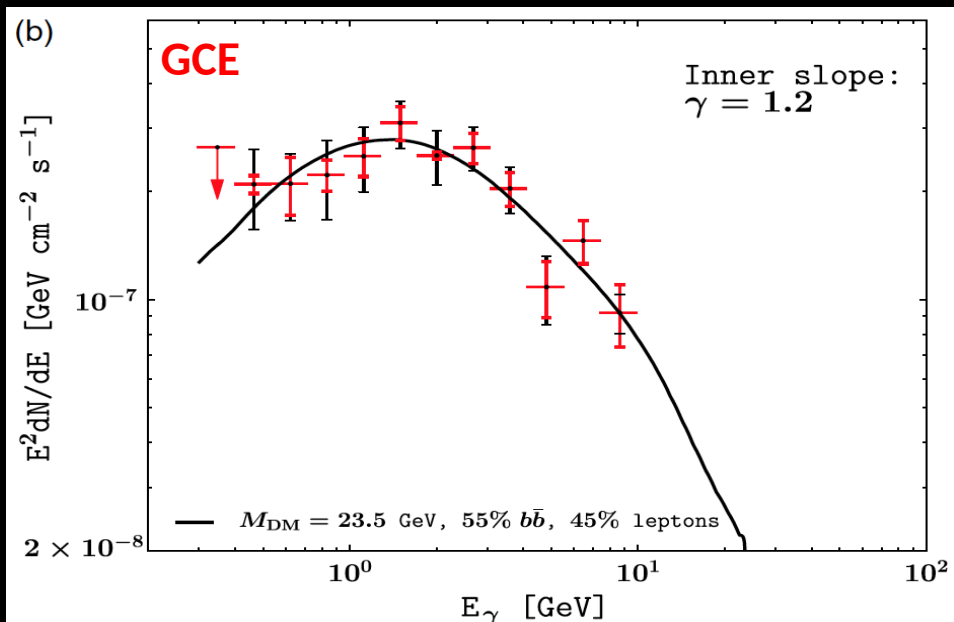
Main features:

- Spectrum peaks at a \sim GeV
- Peak flux $\sim 10^{-(6-7)}$ GeV cm $^{-2}$ s $^{-1}$
- Gamma-ray luminosity is $\sim 10^{36}-10^{37}$ erg/s
- Spatial morphology $\sim r^{-2.4}$

Significance

Statistical significance is $\sim 20-60\sigma$ depending on the data and templates used.

Gordon & Macias (2013)

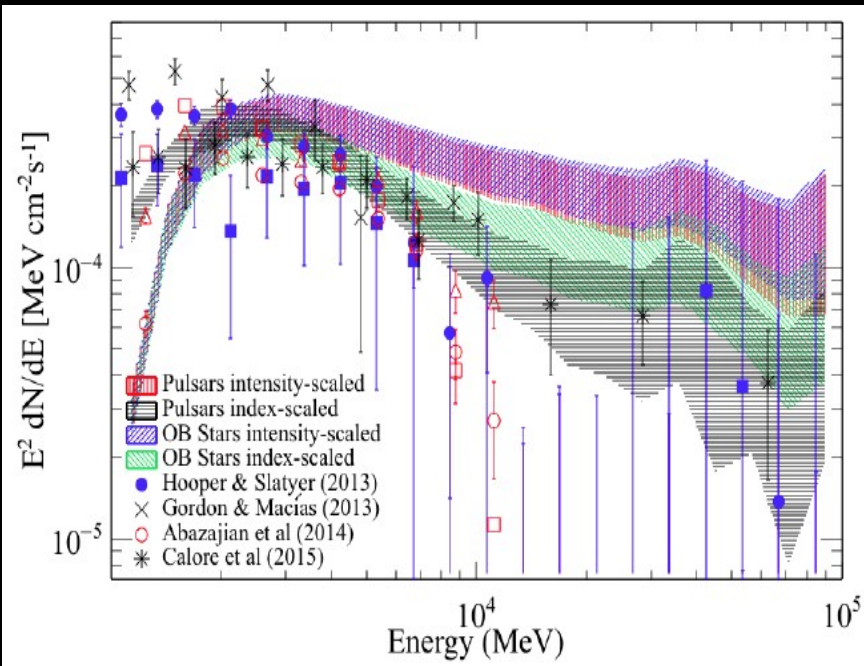


Background model uncertainties

More relevant is systematic uncertainty.

Dedicated diffuse models

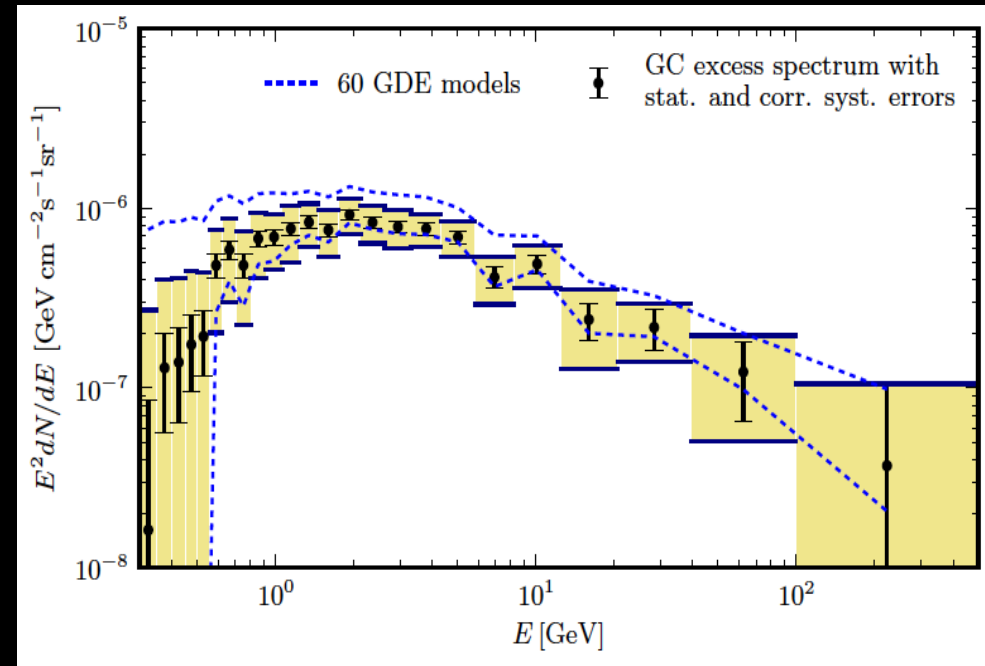
Calibrated by the Fermi collaboration
for Galactic Center analysis



Fermi (2016)

Galprop models

Scan range of parameters of diffusion, B-fields, ISRF, cosmic-ray injection, etc...



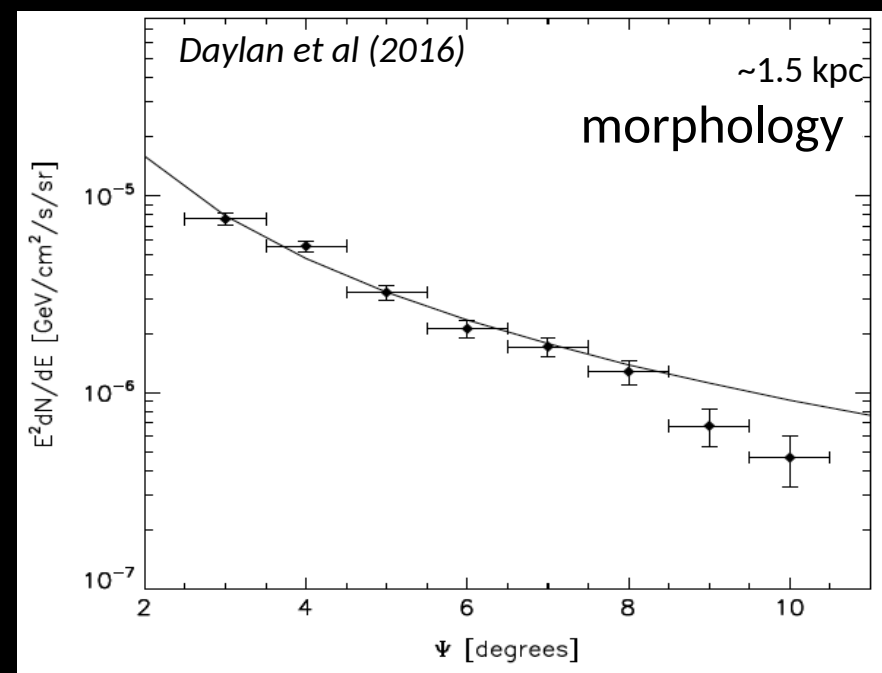
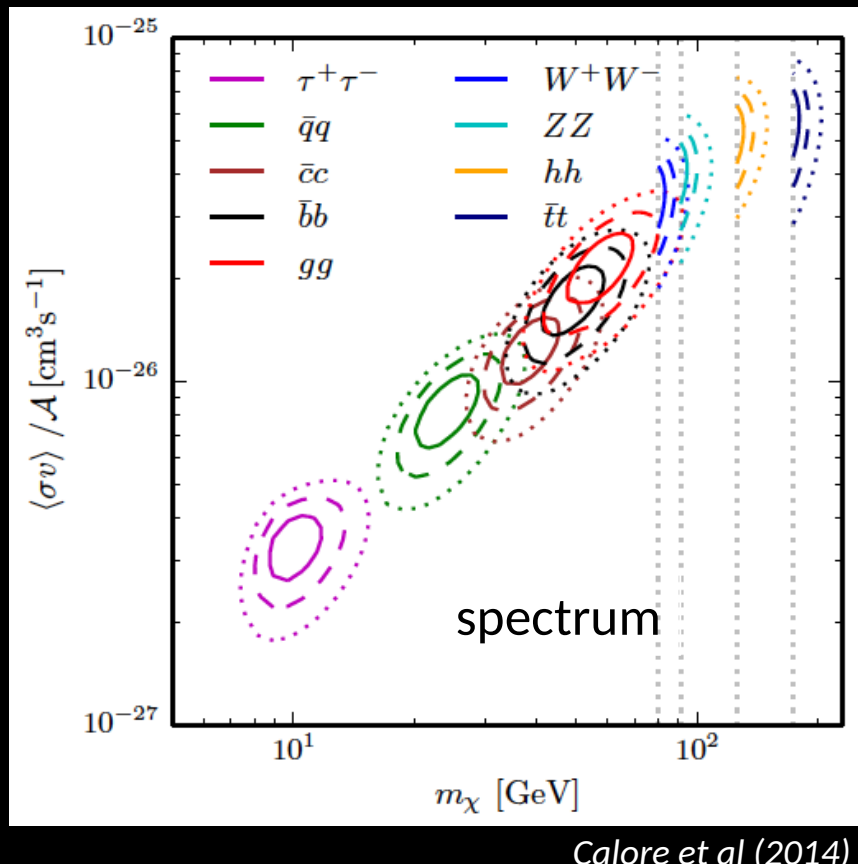
Calore et al (2015)

Despite efforts, the excess remains

Dark Matter

Dark matter can explain the observations

Annihilation of thermally produced WIMPs
explains the spectrum and morphology
well

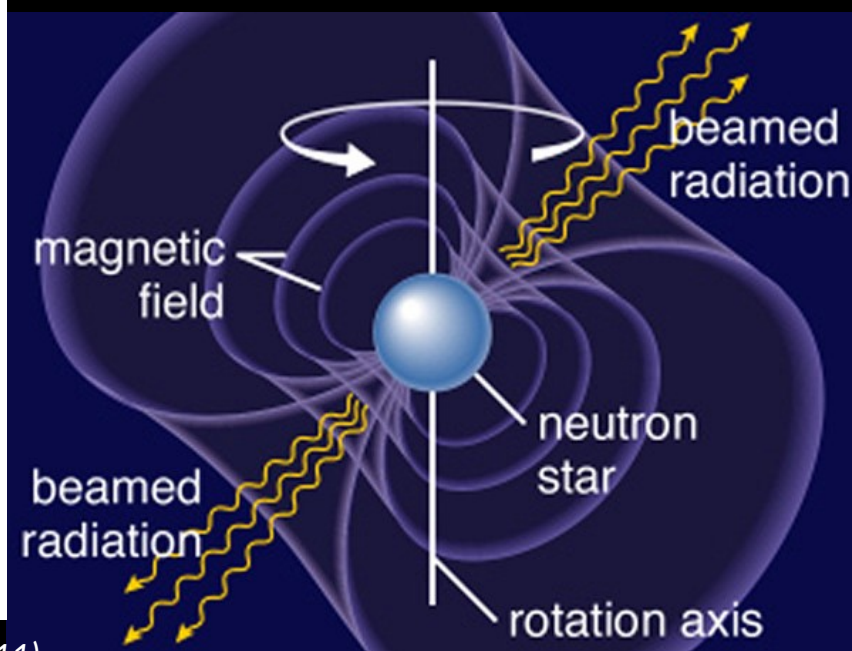
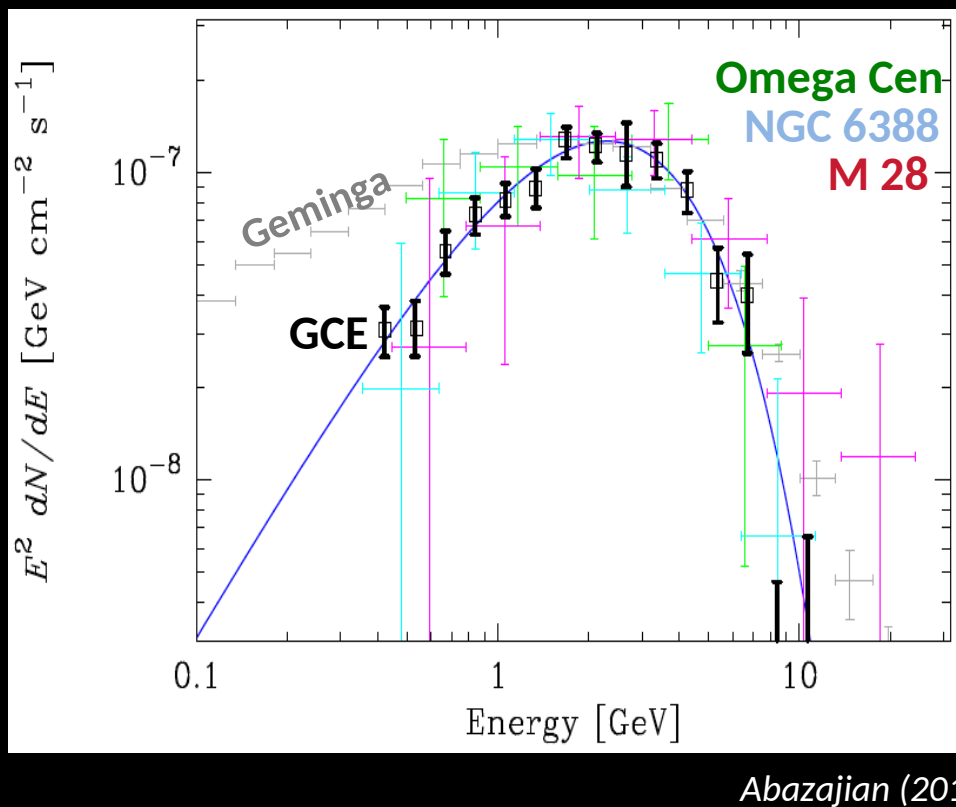
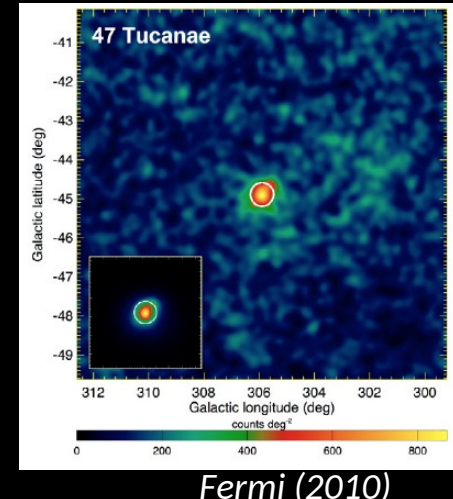


Spectral similarity with millisecond pulsars

Millisecond pulsars

- Millisecond pulsars are gamma-ray sources with similar spectra to the GCE.
- O(5,000) needed in the Galactic Center

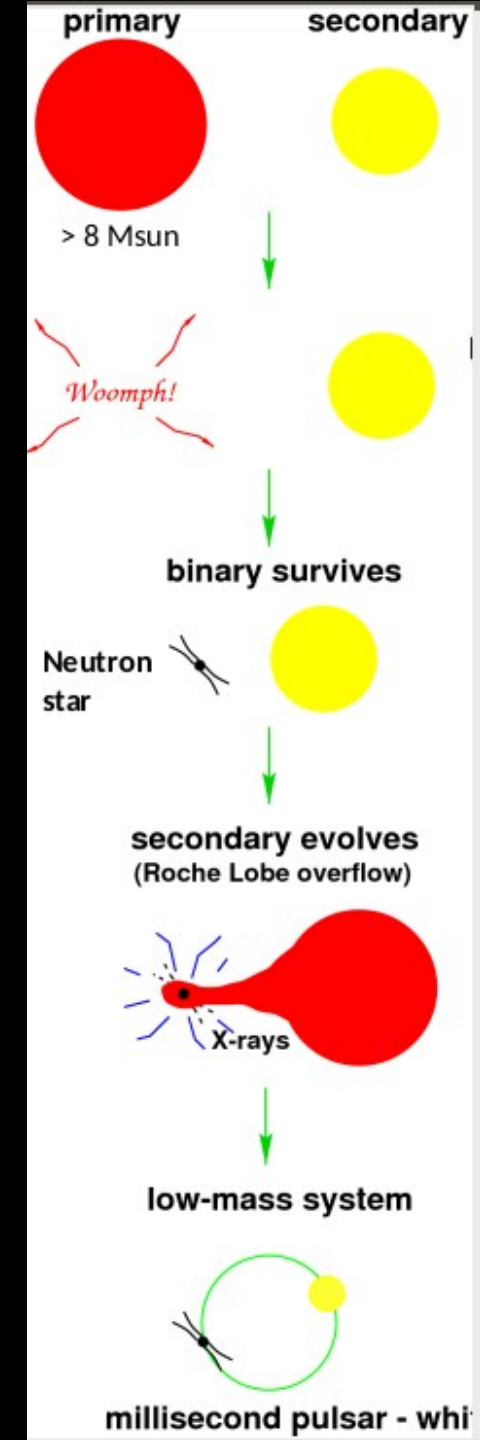
Globular clusters detected in gamma rays



The MSP scenario

Millisecond pulsars:

- Lower B fields than pulsars ($\sim 10^{8-9}$ G vs $\sim 10^{11-13}$ G)
- Lower velocities than pulsars (~ 130 km/s vs ~ 400 km/s)
- Higher birth rate ($\sim 5 \times 10^{-6}$ /yr) than X-ray binaries ($\sim 10^{-7}$ /yr)



Recycling of old neutron stars:

- ✓ Initially a normal NS, but B-field decays or is buried in the superconducting core (resurface must be stopped)
- ? Lower velocities due to binary?
- ? Birth rate not enough, unless X-ray emitting phase is reduced, or population not in steady state
- ✗ X-ray binary phase causes tidal forces that reduce eccentricity

The MSP scenario is rich

MSPs can be formed via a number of channels

- Recycling of old neutron stars
- Accretion induced collapse of O-Ne-Mg white dwarfs
- Merger induced collapse of two white dwarfs

All channels involve binary systems

- Primordial: stars born in binary systems
- Dynamical: captures a companion through encounters

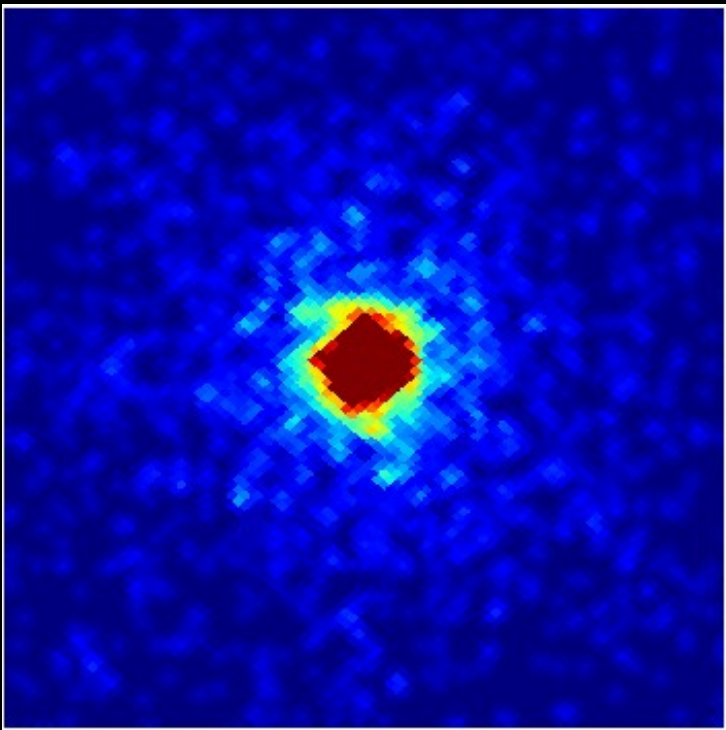
Binary mass transfer and the X-ray connection will be different for different channels.

The relative importance of channels will be environmentally dependent

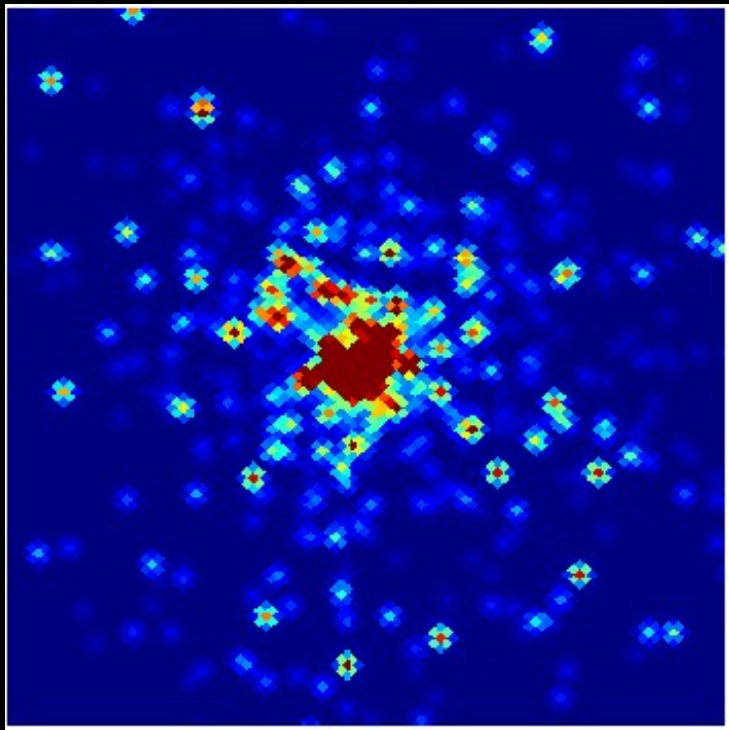
- Stellar age: active star forming (CMZ) to Gyrs old (bulge)
- Stellar density: low (bulge) to high (globular cluster)
- Stellar metallicity: low to solar populations

→ No a priori reason MSP population & their connection to LMXB are the same everywhere

point source vs diffuse source

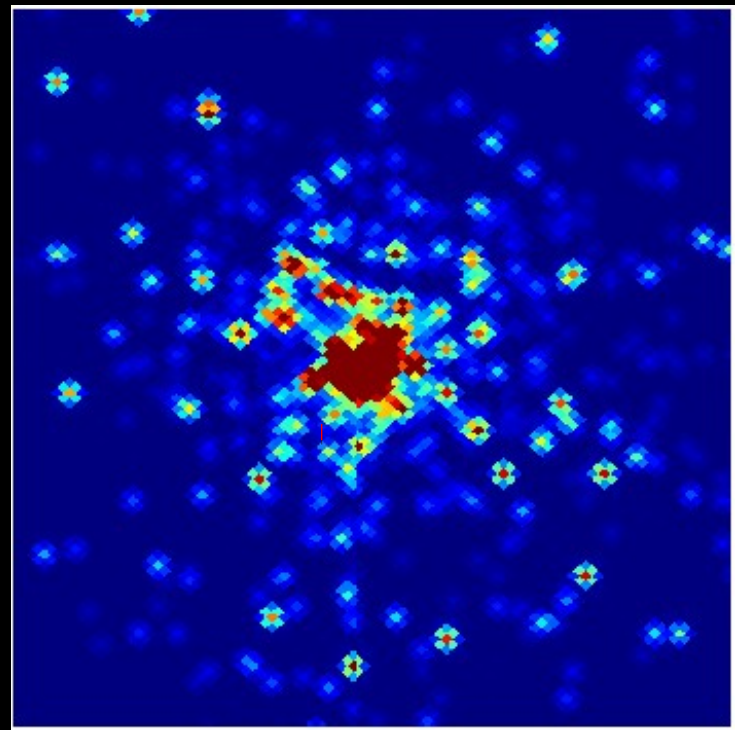
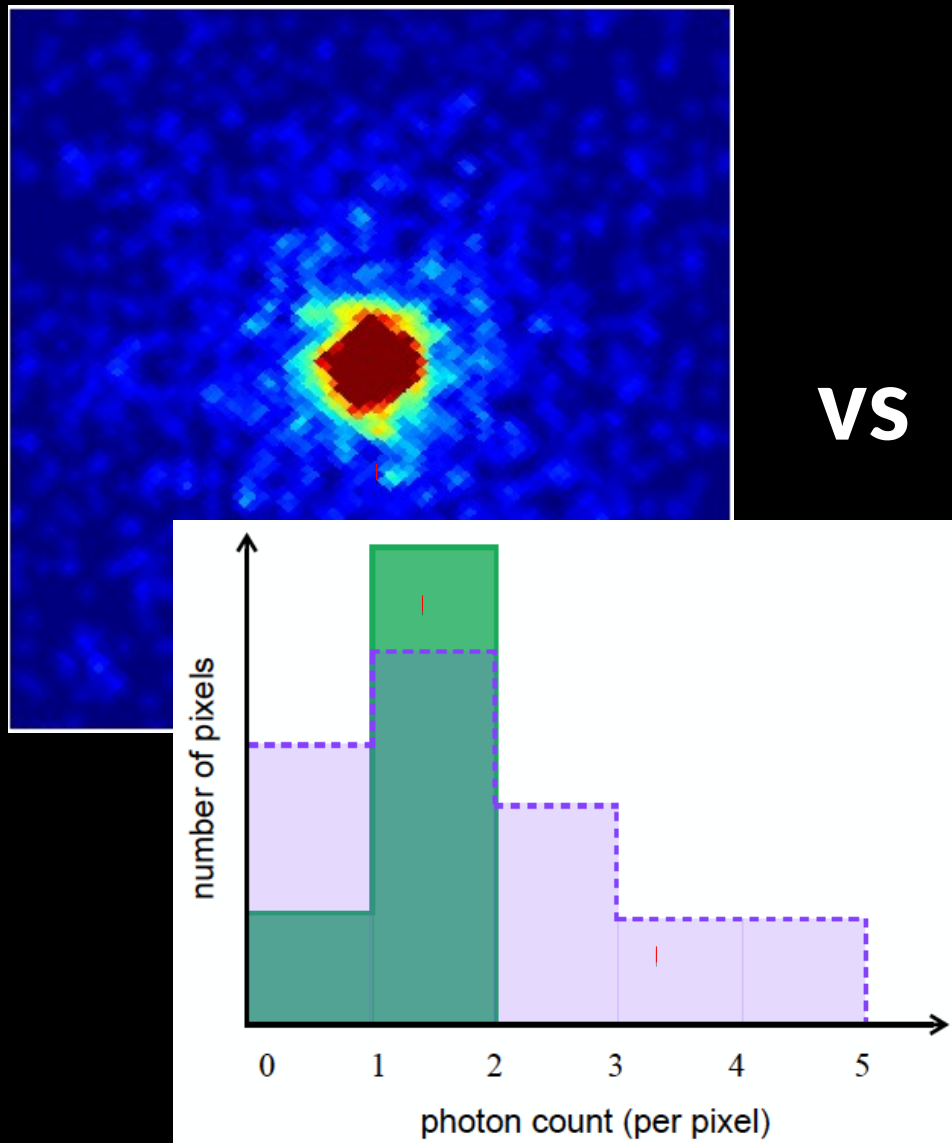


VS



Lee et al (2016)

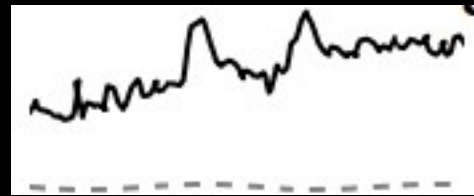
point source vs diffuse source



Lee et al (2016)

Look for peaks on top of Poisson noise
Bartels et al (2016)

data



c.f. P(D) distribution in X-ray astronomy (Malyshev & Hogg 2011)

Photon count distribution fit procedure

Non-Poissonian fit

Fit the photon counts distribution in < 30 deg

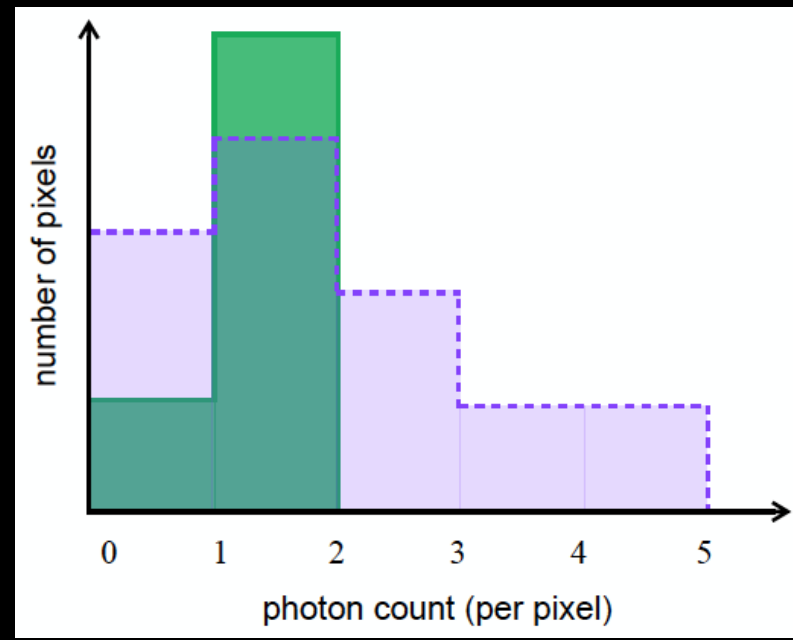
Smooth emission: follows Poisson statistics,
Galactic diffuse, bubbles, isotropic, NFW-DM

$$p_k^{(p)} = \lambda^k e^{-\lambda} / k!$$

λ : Sum of templates

Source count:

$$\frac{dN^{(p)}}{dF} = A^p \begin{cases} \left(\frac{F}{F_b}\right)^{-n_1}, & F \geq F_b \\ \left(\frac{F}{F_b}\right)^{-n_2}, & F < F_b \end{cases}$$



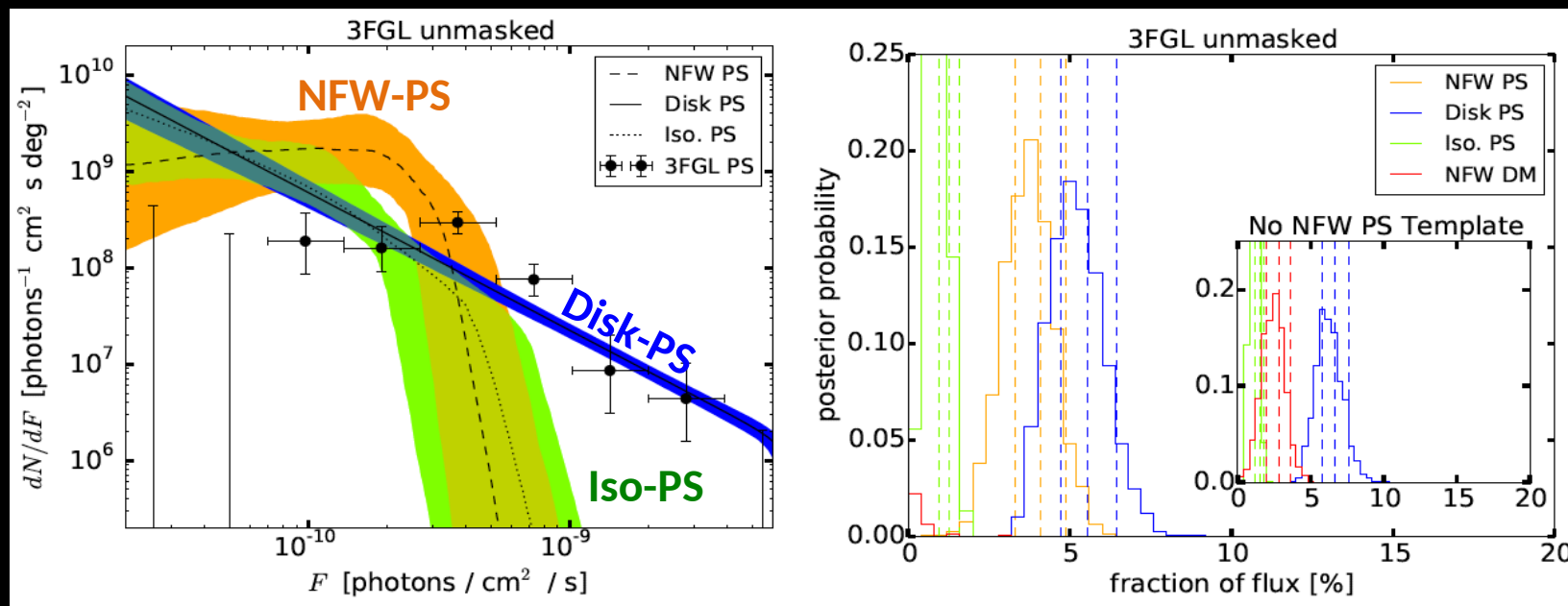
Lee et al (2016)

Where A^p follows the spatial morphology:

- Disk-PS
- NFW-PS
- Extragalactic-PS

Photon count distribution fit result

- NFW-PS contributes $\sim 8.7\%$ of photons, while NFW-DM is consistent with 0%
- Bayes factor 10^6 for NFW-PS compared to without
- If NFW-PS is not added, the NFW-DM absorbs the excess
- The diffuse emission normalization stays within 1% of high latitude values.



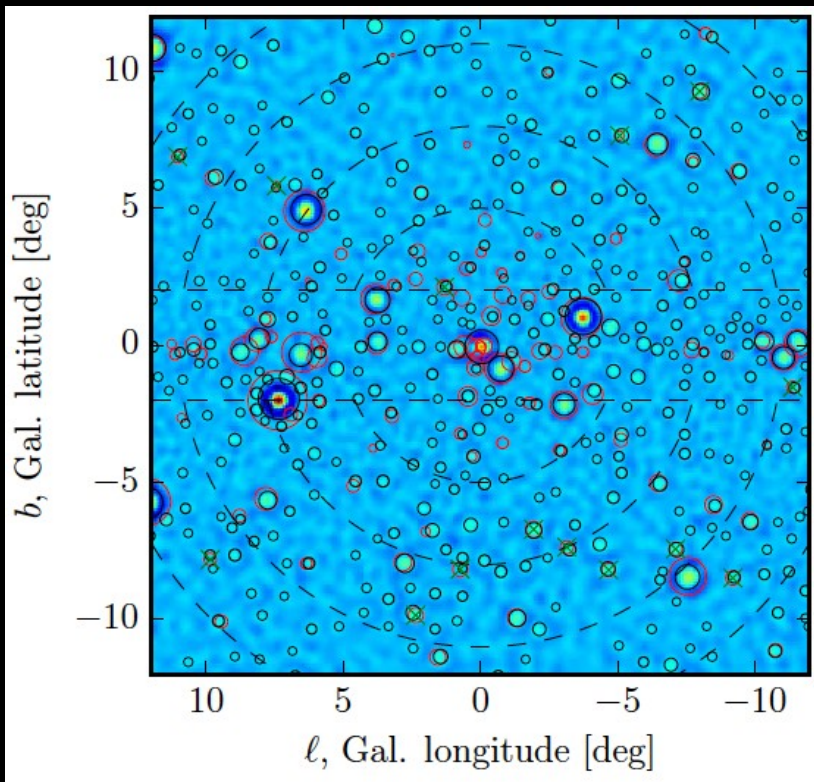
Lee et al (2016)

Strong preference for sub-threshold point sources following the NFW morphology over a diffuse NFW (dark matter) source

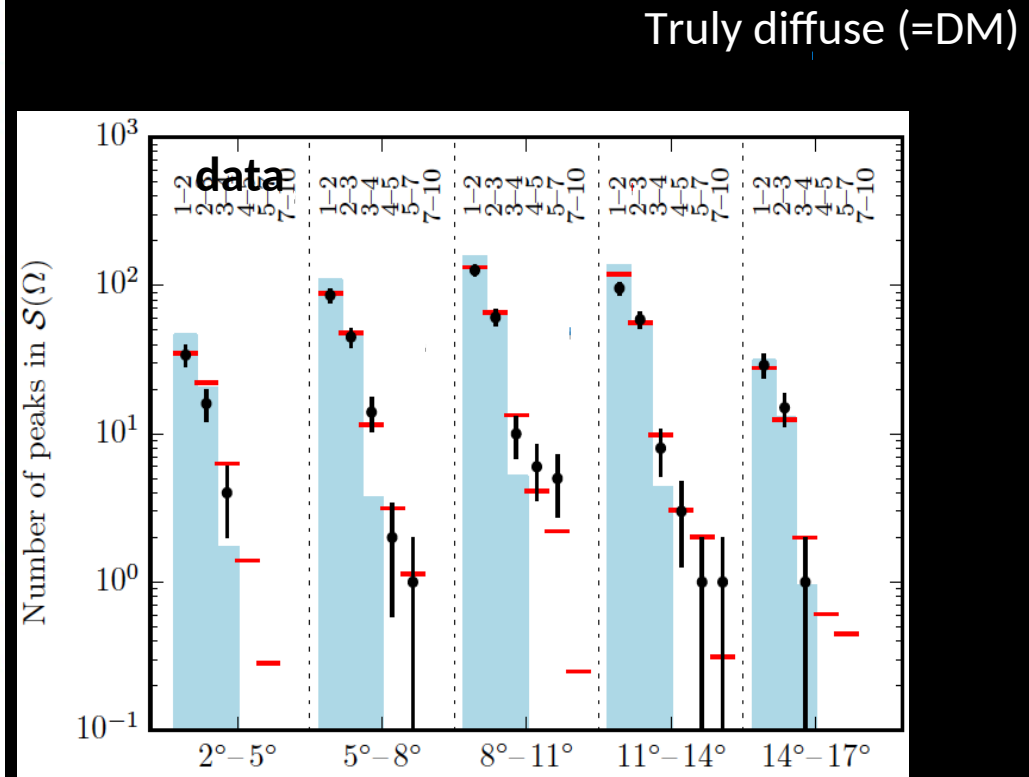
Same conclusions with a wavelet method

Wavelet analysis

1. Convolve with a Mexican hat kernel to identify peaks in high signal-to-noise.
2. Fit better by sub-threshold point sources than diffuse source



Bartels et al (2016)



Point sources (=MSP)

The Stellar Population of the Galactic Bulge



Image credit: ESO

Close to 33% of all Galaxies display a boxy/peanut or X-shape bulge when seen edge on [Jarvis 1986]

The peanut-shaped Stellar Population of the Galactic Bulge

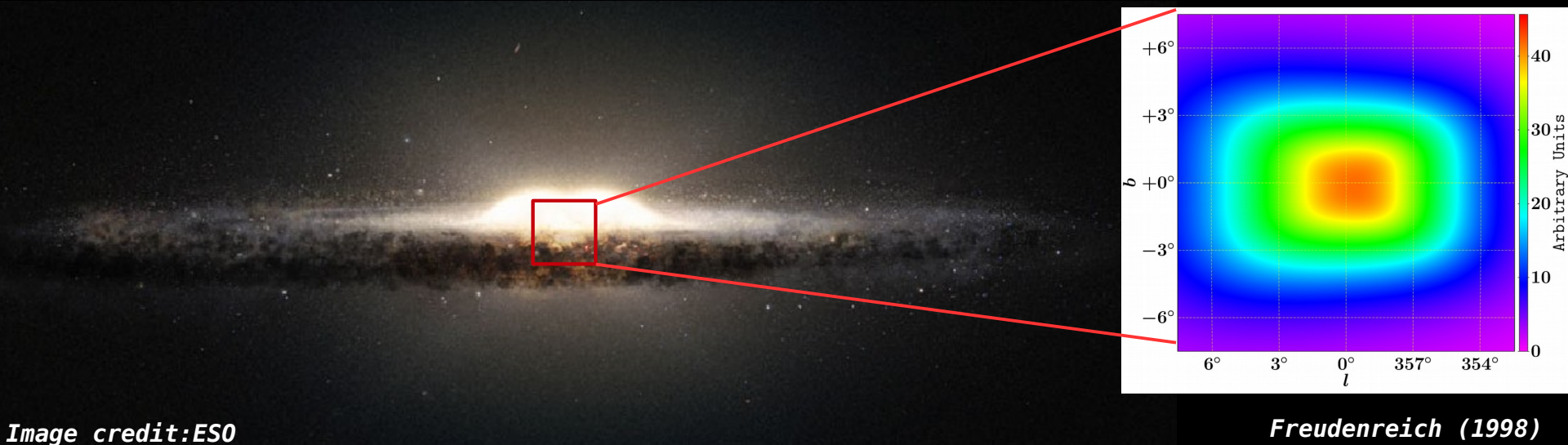


Image credit: ESO

Freudenreich (1998)

→ { There is a peanut shaped excess in infrared emission as seen by the COBE satellite.

The peanut-shaped Stellar Population of the Galactic Bulge

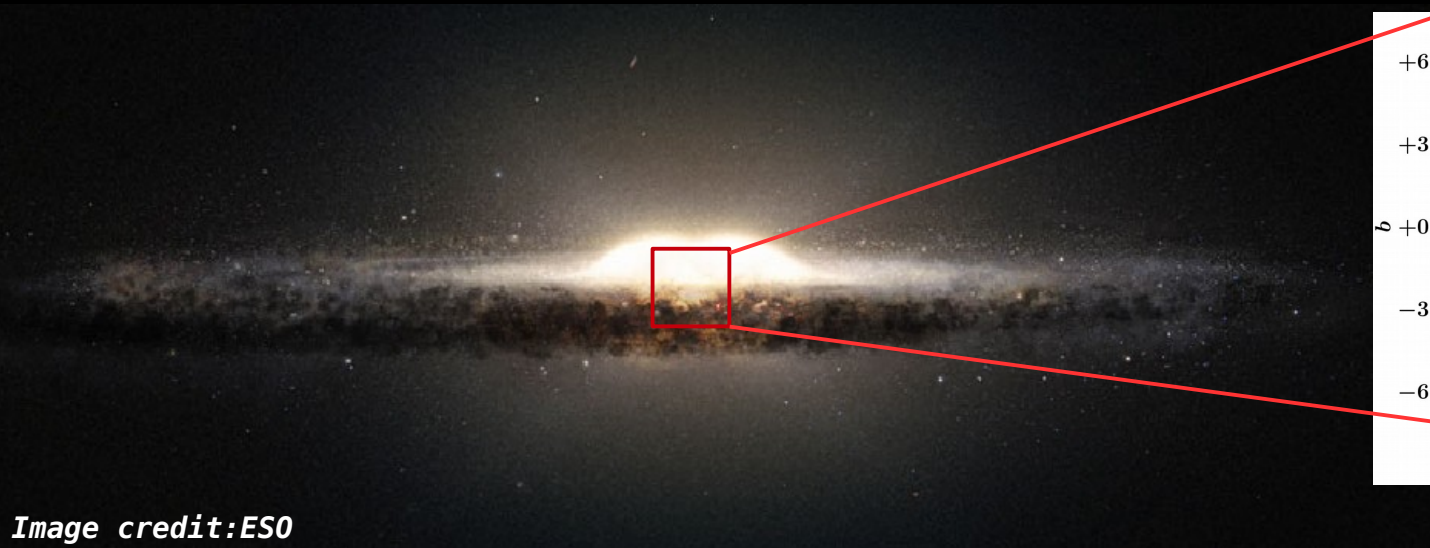
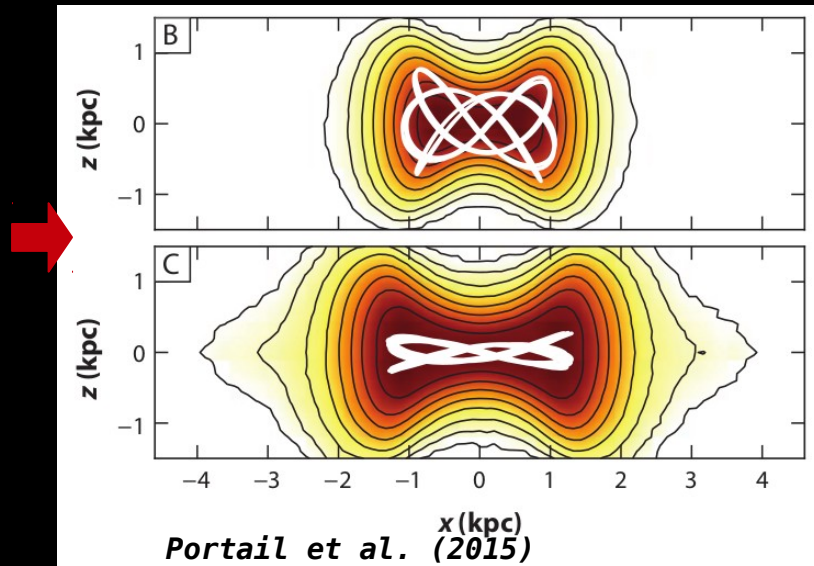


Image credit: ESO

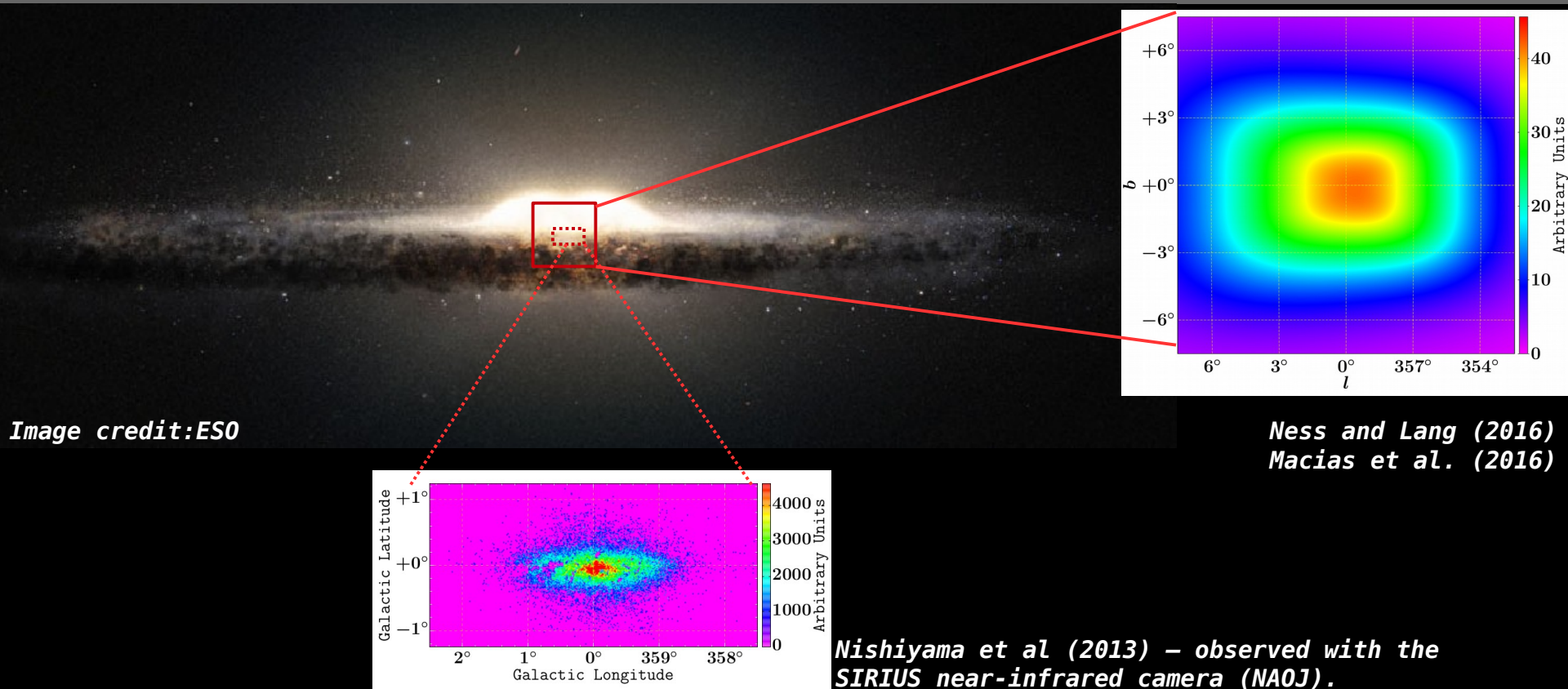
Freudenreich (1998)

Dynamical instabilities of stars in the Galactic bar send these to orbits resembling a peanut shape



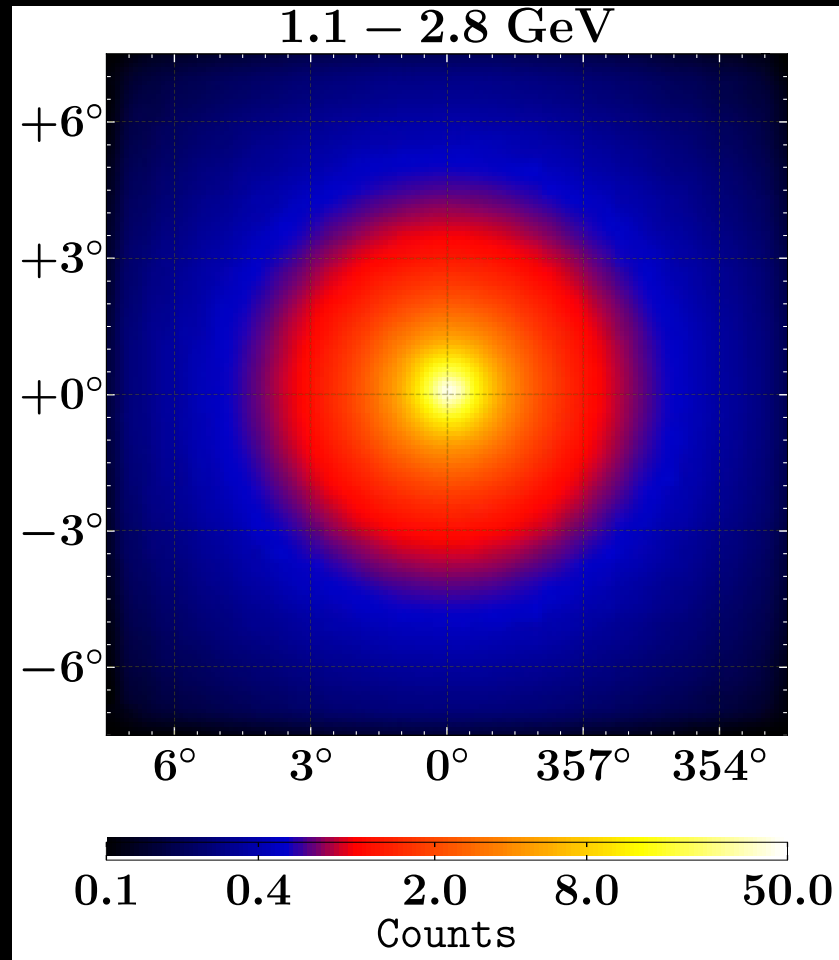
Portail et al. (2015)

The Peanut-shaped Stellar Population of the Galactic Bulge and the Nuclear bulge stars

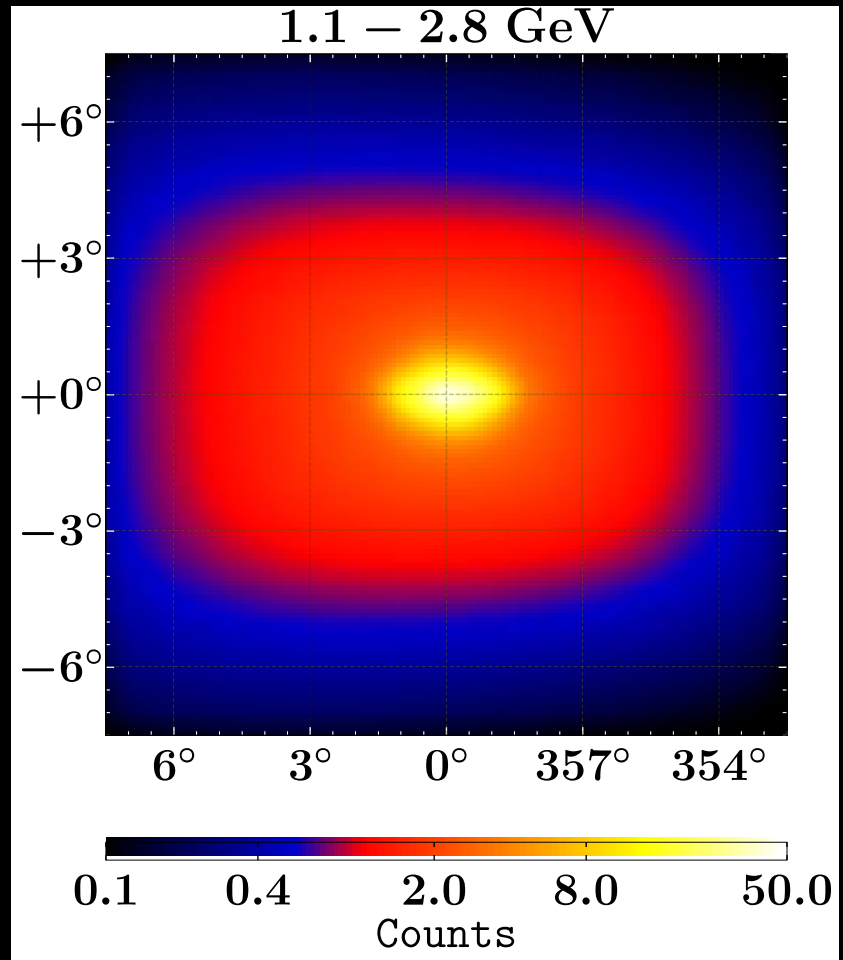


→ There is an additional dense and disky star population close to the supermassive black hole.

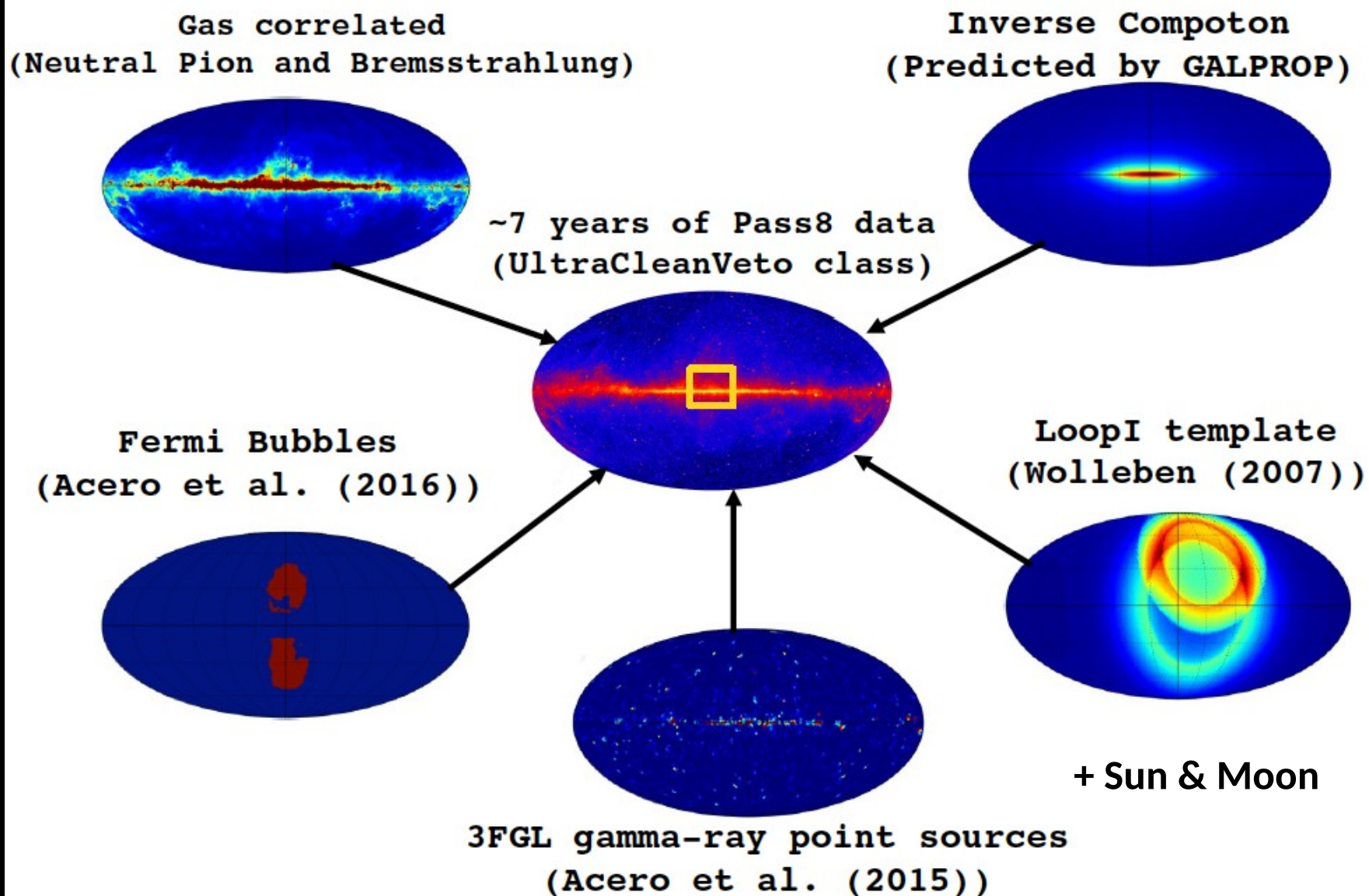
spherical symmetry vs bulge shape



VS



Define a base model



Add new components systematically

Base	Source	$\log(\mathcal{L}_{\text{Base}})$	$\log(\mathcal{L}_{\text{Base+Source}})$	$\text{TS}_{\text{Source}}$	σ	Number of source parameters
baseline baseline baseline baseline baseline baseline baseline	Gas + IC + 3FGL + Loop I + Sun & Moon	FB	-172461.4	-172422.3	78	6.9
		NFW-s	-172461.4	-172265.3	392	18.4
		Boxy bulge	-172461.4	-172238.7	445	19.7
		X-bulge	-172461.4	-172224.1	475	20.5
		NFW	-172461.4	-172167.9	587	23.0
		NB	-172461.4	-171991.8	939	29.5
		NP	-172461.4	-169804.1	5315	55.7
baseline	NP	FB	-169804.1	-169773.6	61	5.8
baseline	NP	NB	-169804.1	-169697.2	214	13.0
baseline	NP	Boxy bulge	-169804.1	-169663.7	281	15.3
baseline	NP	NFW	-169804.1	-169623.3	362	17.6
baseline	NP	X-bulge	-169804.1	-169616.2	376	18.0
baseline+NP+Boxy bulge	NFW	Boxy bulge	-169663.7	-169598.2	131	9.7
baseline+NP+Boxy bulge	NB	Boxy bulge	-169663.7	-169566.0	195	12.4
baseline+NP+Boxy bulge	NB	NFW	-169566.0	-169553.3	25	2.7
baseline+NP+Boxy bulge	NFW	NB	-169598.2	-169553.3	90	7.6
baseline+NP+NFW	Boxy bulge+NB	Boxy bulge+NB	-169623.3	-169553.0	140	10.0
baseline+NP+NFW	X-bulge+NB	X-bulge+NB	-169623.3	-169531.0	185	10.8
baseline+NP+NB	X-bulge	X-bulge	-169697.2	-169542.0	310	16.1
baseline+NP+NB	Boxy bulge	Boxy bulge	-169697.2	-169566.0	262	14.6
baseline+NP+NB	NFW	NFW	-169697.2	-169599.0	197	12.4
baseline+NP+NB+NFW	X-bulge	X-bulge	-169598.9	-169531.0	136	9.9
baseline+NP+X-bulge+NB	NFW	NFW	-169542.0	-169531.0	22	2.4

Macias et al (2018)

NFW detected at low significance when bulge is included

Add new components systematically

Base	Source	$\log(\mathcal{L}_{\text{Base}})$	$\log(\mathcal{L}_{\text{Base+Source}})$	$\text{TS}_{\text{Source}}$	σ	Number of source parameters
baseline + Gas + IC + 3FGL + Loop I + Sun & Moon	FB	-172461.4	-172422.3	78	6.9	19
	NFW-s	-172461.4	-172265.3	392	18.4	19
	Boxy bulge	-172461.4	-172238.7	445	19.7	19
	X-bulge	-172461.4	-172224.1	475	20.5	19
	NFW	-172461.4	-172167.9	587	23.0	19
	NB	-172461.4	-171991.8	939	29.5	19
	NP	-172461.4	-169804.1	5315	55.7	64×19
baseline + NP	FB	-169804.1	-169773.6	61	5.8	19
baseline + NP	NB	-169804.1	-169697.2	214	13.0	19
baseline + NP	Boxy bulge	-169804.1	-169663.7	281	15.3	19
baseline + NP	NFW	-169804.1	-169623.3	362	17.6	19
baseline + NP	X-bulge	-169804.1	-169616.2	376	18.0	19
baseline + NP + Boxy bulge	NFW	-169663.7	-169598.2	131	9.7	19
baseline + NP + Boxy bulge	NB	-169663.7	-169566.0	195	12.4	19
baseline + NP + Boxy bulge + NB	NFW	-169566.0	-169553.3	25	2.7	19
baseline + NP + Boxy bulge + NFW	NB	-169598.2	-169553.3	90	7.6	19
baseline + NP + NFW	Boxy bulge + NB	-169623.3	-169553.0	140	10.0	2×19
baseline + NP + NFW	X-bulge + NB	-169623.3	-169531.0	185	10.8	2×19
baseline + NP + NB	X-bulge	-169697.2	-169542.0	310	16.1	19
baseline + NP + NB	Boxy bulge	-169697.2	-169566.0	262	14.6	19
baseline + NP + NB	NFW	-169697.2	-169599.0	197	12.4	19
baseline + NP + NB + NFW	X-bulge	-169598.9	-169531.0	136	9.9	19
baseline + NP + X-bulge + NB	NFW	-169542.0	-169531.0	22	2.4	19

Macias et al (2018)

NFW detected at low significance when bulge is included

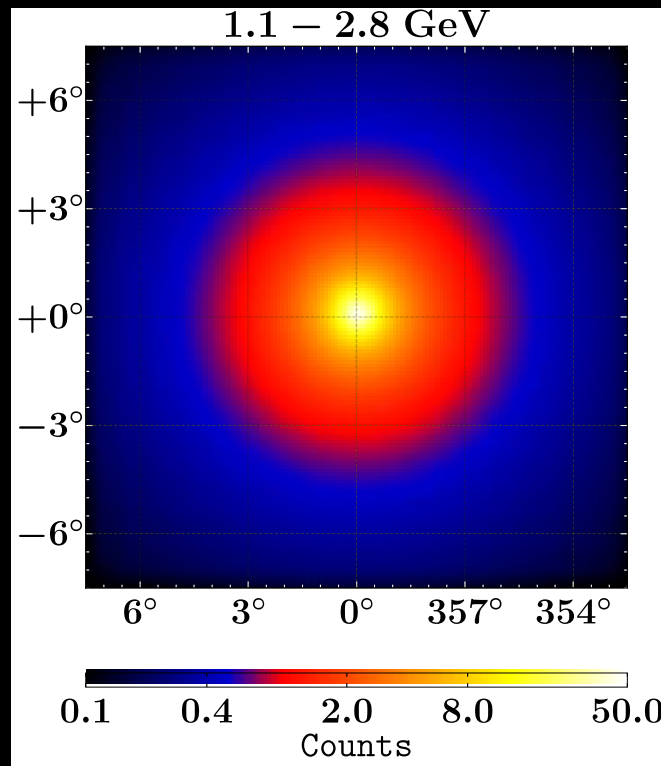
Bulge preferred over spherical symmetry

Bulge over NFW

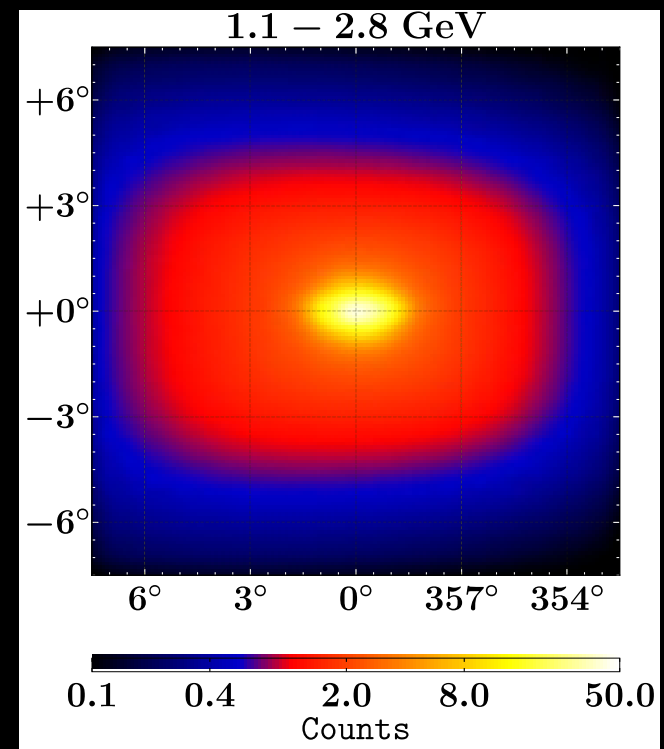
When a bulge model is included, the detection of NFW² falls ($\sigma < 3$) while bulge significance is $\sigma > 10$.

This is robust to

- Point sources used
- Diffuse emission models used
- Galactic mask



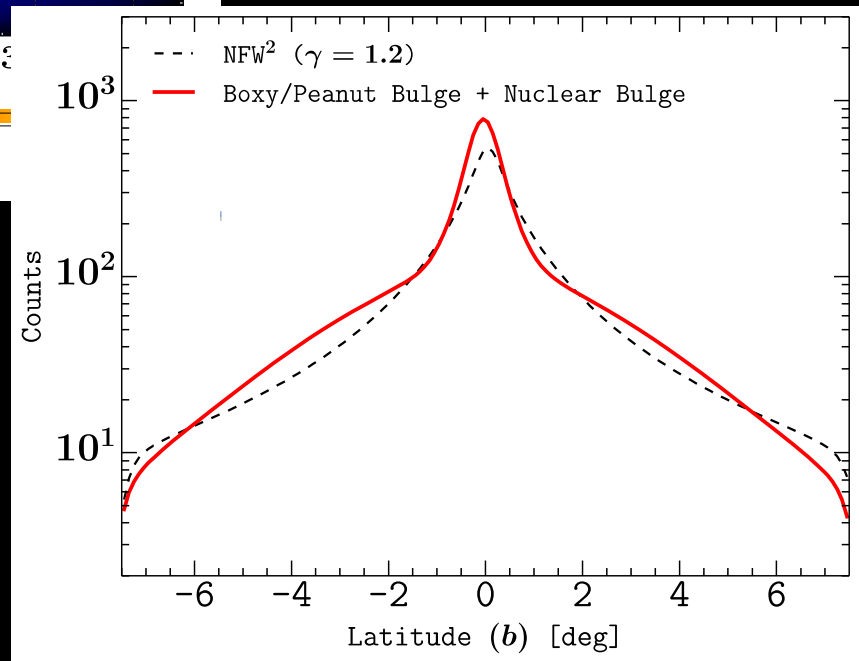
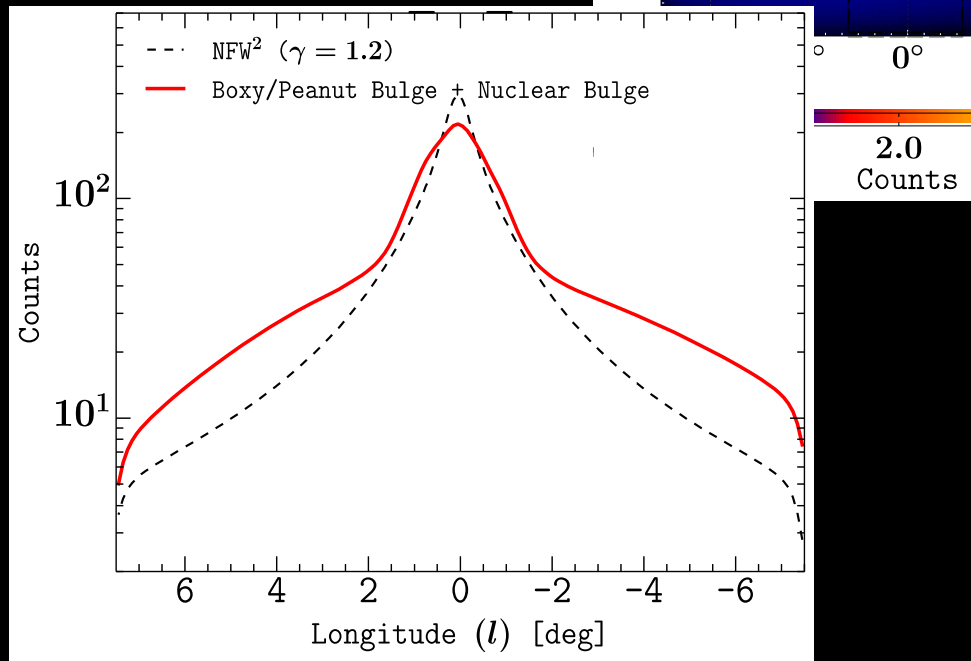
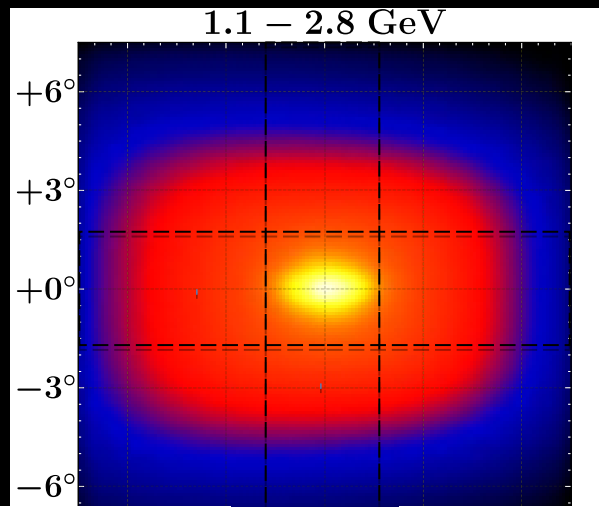
<<



Difficulties of dark matter: morphology

Bulge over NFW

The data prefers an asymmetric excess outside of several degrees (the central few degrees are NFW-like)



SkyFACT : a hybrid approach

Storm et al (2017)

SkyFACT = **S**ky **F**actorization with **A**daptive **C**onstrained **T**emplates

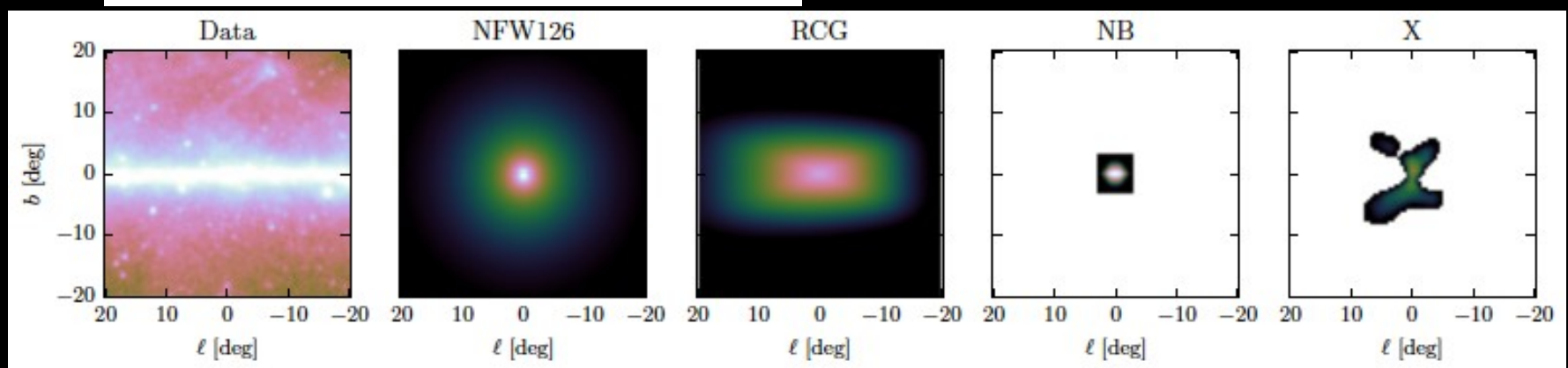
Hybrid method to study diffuse gamma rays that combines adaptive spatial-spectral template regression and image reconstruction.

Spatial template

Spectral template

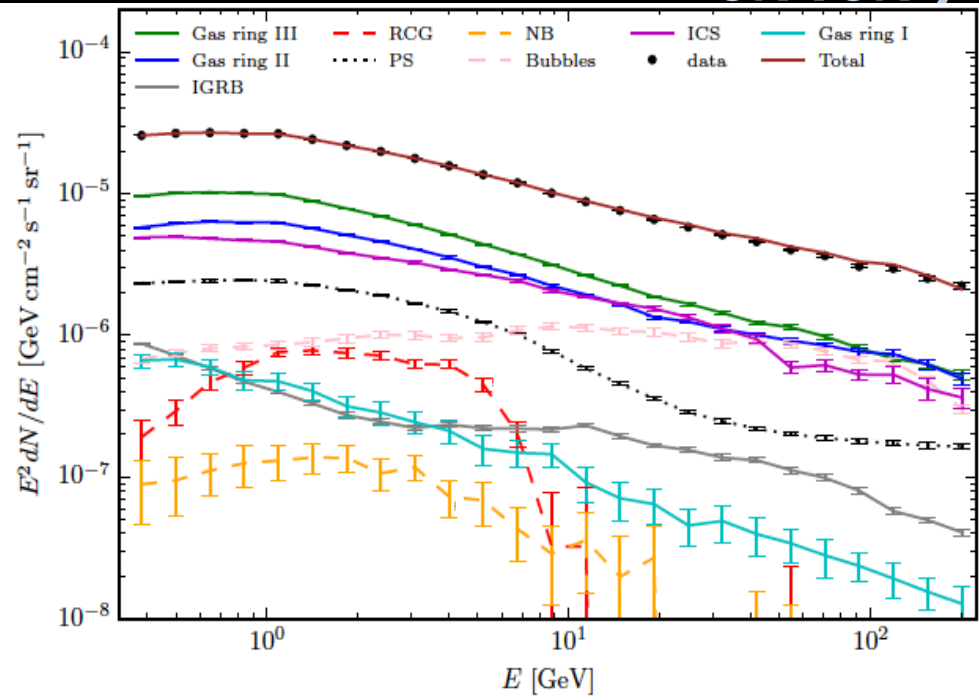
$$\phi_{pb} = \sum_k T_p^{(k)} \tau_p^{(k)} \cdot S_b^{(k)} \sigma_b^{(k)} \cdot \nu^{(k)}$$

Modulated by nuisance parameters τ , σ , ν



Bartels et al (2017)

Same conclusions from SkyFACT analysis



Fit in central 40x180 degrees, which facilitates the fitting of gas template rings (x3) and provides leverage to disentangle components.

- Boxy bulge
- Nuclear bulge

We demonstrated that the stellar bulge model provides a significantly better fit ($> 10\sigma$) to the data than the DM-emission related Einasto or contracted NFW profiles. Hence the GCE appears to simply trace stellar mass in the bulge, not the dark matter density squared (although the actual DM profile is sufficiently uncertain that this possibility cannot be entirely excluded). What

What have we learned so far?

1) Spectrum of the Galactic Center Excess?



Agrees well with spectrum of millisecond pulsars in Globular clusters

2) Spatial Morphology of the GCE?



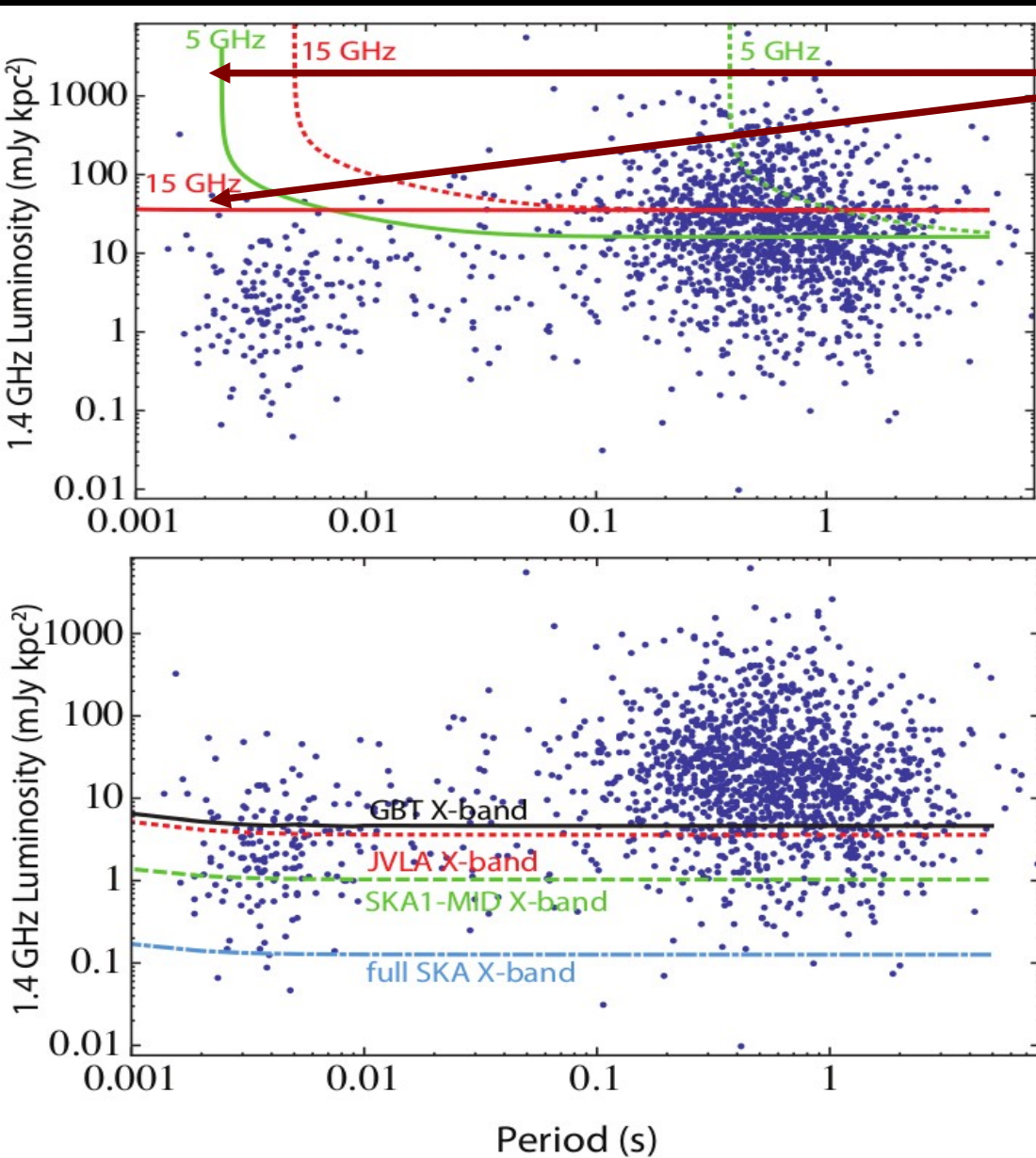
Follows the distribution of stars in the Galactic bulge

3) Photon statistics?



Well described by non-Poissonian templates, which suggests an unresolved population of point sources in the GC.

How to detect the individual Millisecond Pulsars?



10 sigma sensitivities of previous 5 GHz and 15 GHz GBT searches at the GC

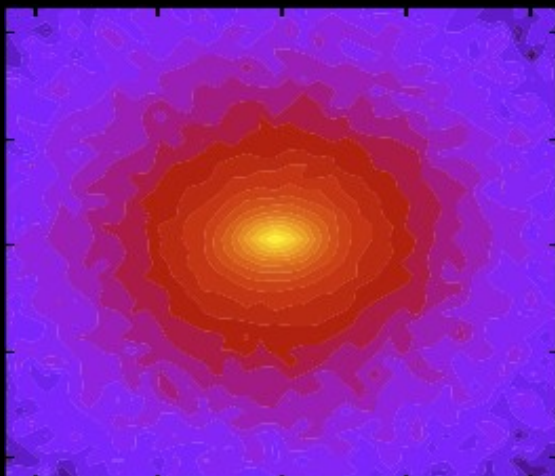
Deep X-band observations of GBT and VLA would be sensitive to a significant fraction of the known MSP population if located at the GC distance.

A dark matter bulge?

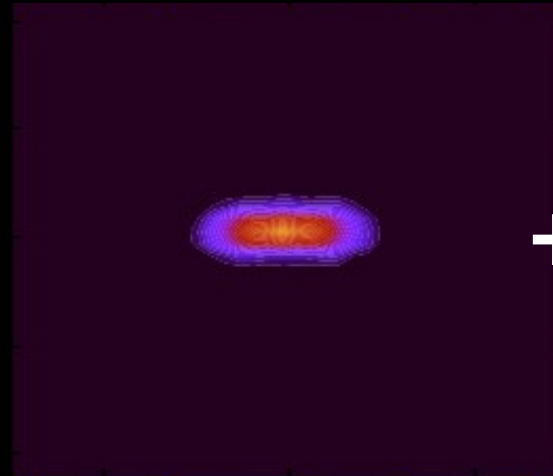
Can dark matter explain the bulge-correlated gamma-ray emission?

Co-evolution of dark matter and disk stars during bar formation:

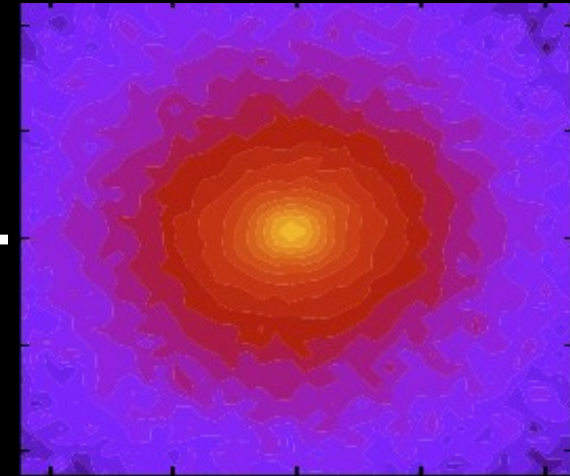
Dark matter



Trapped component



Untrapped component



~12 % of dark matter within bar radius (3kpc) is trapped in the bar

Petersen et al (2016)

→ CDM can form a bulge-like feature, but appears to be subdominant

Thanks!

Back up slides

An unresolved population of Millisecond pulsars traced by the peanut bulge and nuclear bulge could explain the Fermi GeV excess

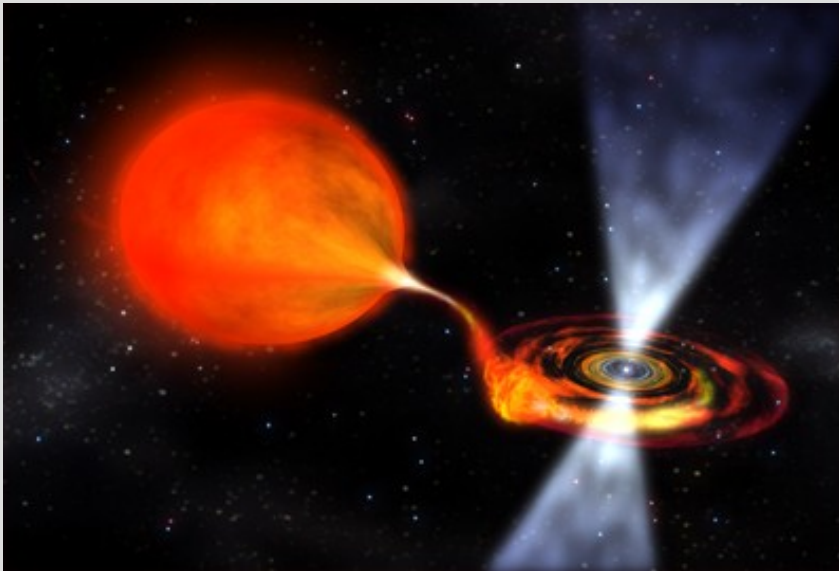


Image Credit: NASA/Dana Berry.

Luminosity-to-mass ratio

Entire Galaxy → $\sim 2 \times 10^{27} \text{ erg/s}/M_{\odot}$

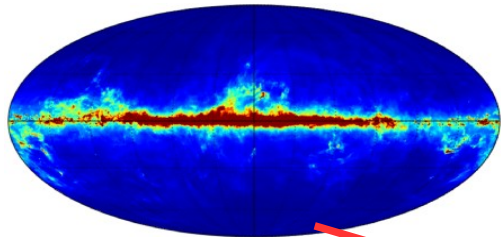
Galactic bulge → $\sim 3 \times 10^{27} \text{ erg/s}/M_{\odot}$

47 Tuc → $\sim 5 \times 10^{28} \text{ erg/s}/M_{\odot}$

Template fitting method

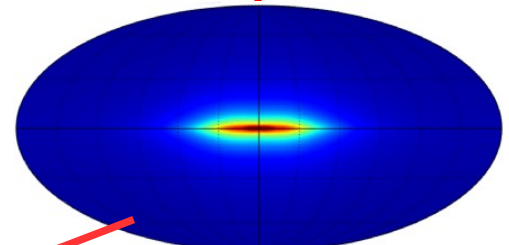
Interstellar gas maps

(Hydrodynamical and Interpolated)



Inverse Compton

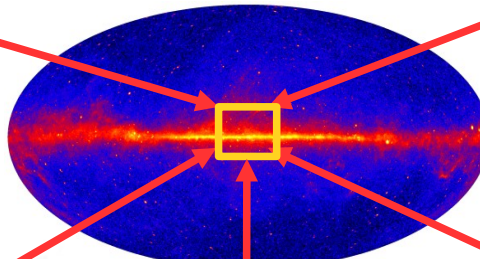
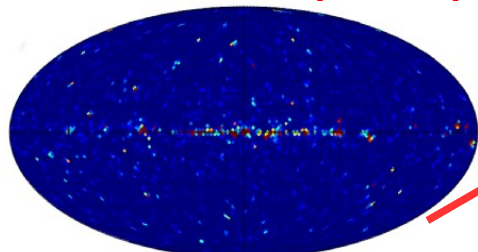
(Predicted by GALPROP)



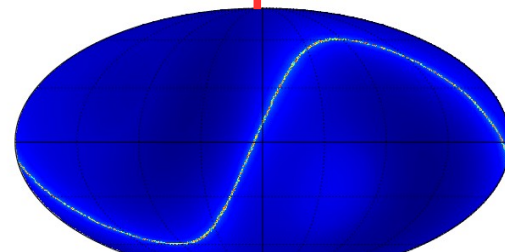
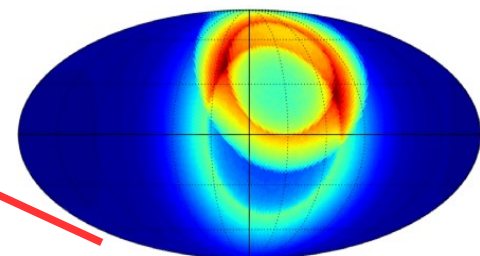
~7 years of Pass8 data
(UltraCleanVeto class)

3FGL sources

(Acero et al. (2015))



LoopI template
(Wolleben (2007))

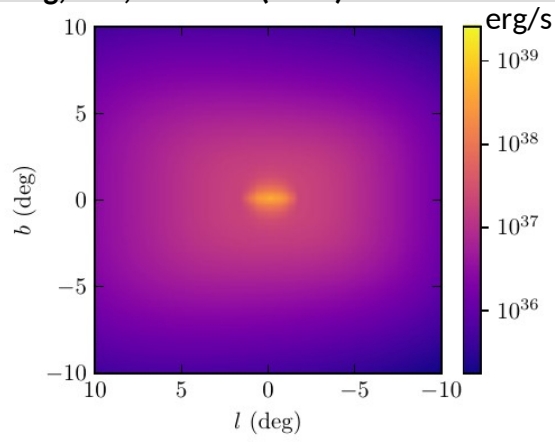


Sun & Moon templates

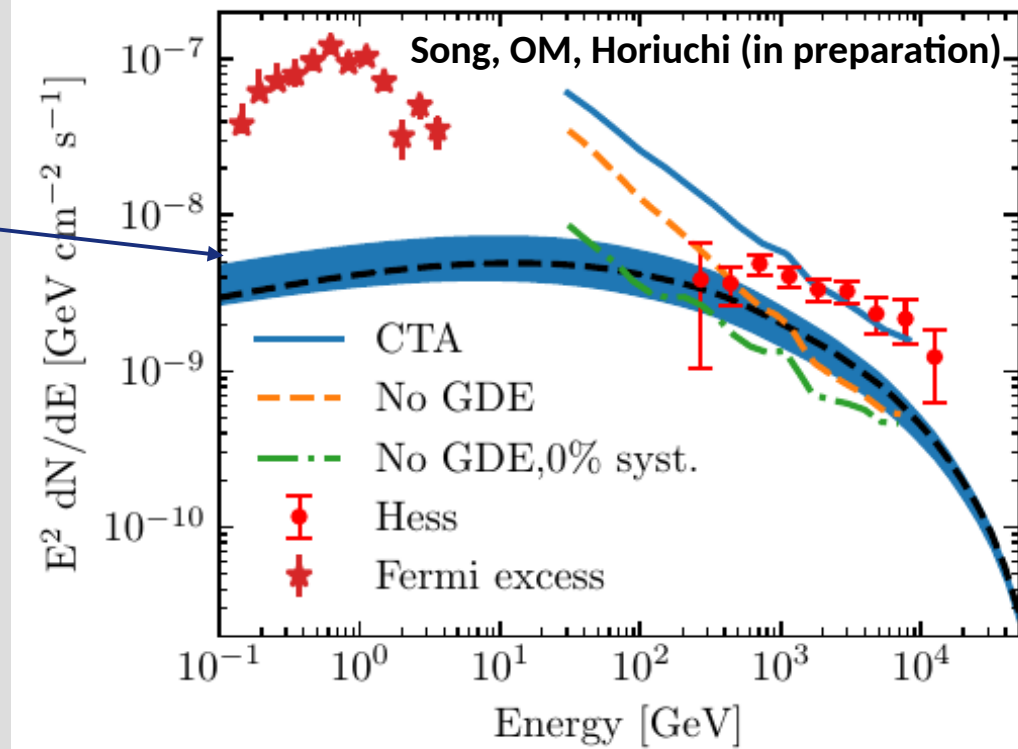
(Generated with the *gtsuntemp* tool – *FermiTools*)

CR electrons from MSPs could produce TeV gamma-ray signals

Song, OM, Horiuchi (2019)



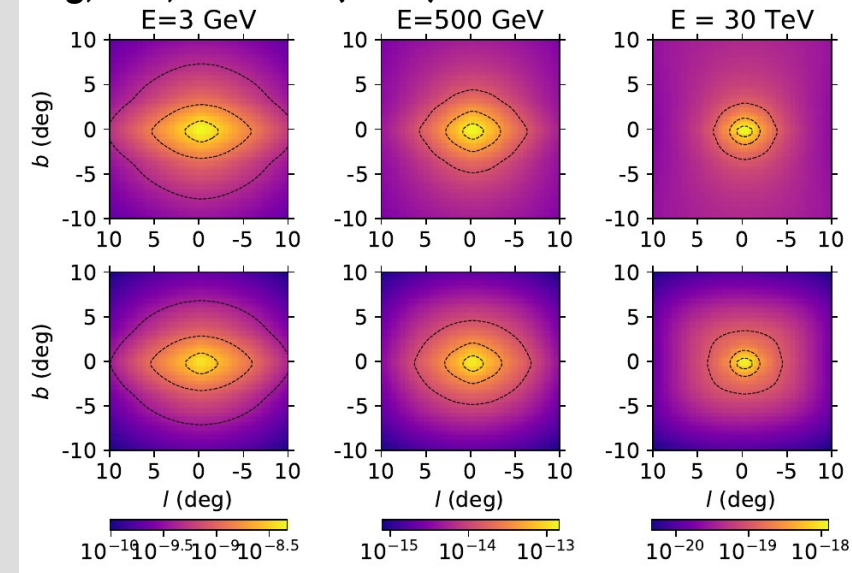
Cosmic Ray electron injection morphology



Inverse Compton spectrum of MSPs electrons.

Spatial morphology of MSPs Inverse Compton emission

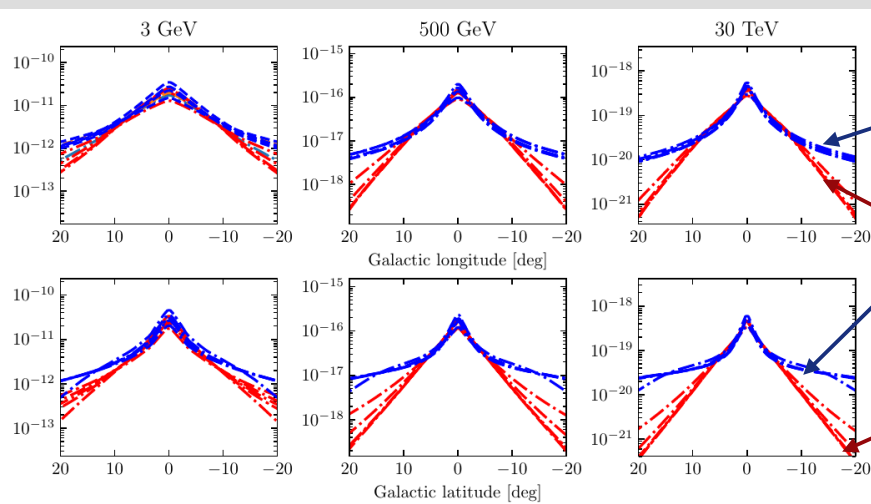
Song, OM, Horiuchi (2019)



Inverse Compton from MSPs
following spherical distribution



Inverse Compton from MSPs
following a peanut bulge
distribution



Spherical distribution

Peanut bulge distribution



Detection Threshold

In our bin-by-bin analysis we had 19 energy bands in each of which the point source amplitude was not allowed to take on a negative value, we thus have a mixture distribution given by

$$p(\text{TS}) = \frac{\delta(\text{TS}) + \sum_{i=1}^{19} \binom{19}{i} \chi_{i+2}^2(\text{TS})}{\sum_{i=0}^{19} \binom{19}{i}}$$

To work out the number of σ of a detection we evaluate the equivalent p-value for a one new parameter case:

$$\text{Number of } \sigma \equiv \sqrt{\text{InverseCDF} \left(\chi_1^2, \text{CDF} \left[p(\text{TS}), \hat{\text{TS}} \right] \right)}$$

For 19 d.o.f a 4 σ detection corresponds to TS>41.8.